Reduced expression of C/EBPβ-LIP extends health- and lifespan in mice

Christine Müller[1,2$], Laura M. Zidek[2$], Tobias Ackermann[1,2], Tristan de Jong[1], Peng Liu[3], Verena Kliche[2], Mohamad Amr Zaini[1,2], Gertrud Kortman[1], Liesbeth Harkema[4], Dineke S. Verbeek[5], Jan P. Tuckermann[3], Julia von Maltzahn[2], Alain de Bruin[4,5], Victor Guryev[1], Zhao-Qi Wang[2] and Cornelis F. Calkhoven[1,2*]

[1] European Research Institute for the Biology of Ageing, University Medical Centre Groningen, University of Groningen, Antonius Deusinglaan 1, NL-9700 AD Groningen, the Netherlands.

[2] Leibniz Institute on Aging - Fritz Lipmann Institute, Beutenbergstrasse 11, D-07745 Jena, Germany.

[3] Institute for Comparative Molecular Endocrinology, University of Ulm, Helmholzstraße 8/1 D-89081 Ulm, Germany.

[4] Dutch Molecular Pathology Centre, Faculty of Veterinary Medicine, Utrecht University, Yalelaan 1, NL-3584 CL Utrecht, the Netherlands.

[5] Department of Genetics, University Medical Center Groningen, University of Groningen, Antonius Deusinglaan 1, NL-9700 RB Groningen, the Netherlands.

[$] These authors contributed equally to this work.

* Corresponding author: c.f.calkhoven@umcg.nl

Abstract

Ageing is associated with physical decline and the development of age-related diseases such as metabolic disorders and cancer. Few conditions are known that attenuate the adverse effects of ageing, including calorie restriction (CR) and reduced signalling through the mechanistic target of rapamycin complex 1 (mTORC1) pathway. Synthesis of the metabolic transcription factor C/EBPβ-LIP is stimulated by mTORC1, which critically depends on a short upstream open reading frame (uORF) in the C/EBPβ-mRNA. Here we describe that reduced C/EBPβ-LIP expression due to genetic ablation of the uORF delays the development of age-associated phenotypes in mice. Moreover, female C/EBPβ$^{\Delta uORF}$ mice display an extended lifespan. Since LIP levels increase upon aging in wt mice, our data reveal an important role for C/EBPβ in the aging process and suggest that restriction of LIP expression sustains health and fitness. Thus, therapeutic strategies targeting C/EBPβ-LIP may offer new possibilities to treat age-related diseases and to prolong healthspan.

Introduction

Delaying the occurrence of age related-diseases and frailty (disabilities) and thus prolonging healthspan, would substantially increase the quality of life of the ageing population and could help to reduce healthcare costs. Calorie restriction (CR) or pharmacological inhibition of the mTORC1 pathway by rapamycin are considered as potential effective interventions to delay aging and to increase healthspan in different species (Kaeberlein, Rabinovitch, & Martin, 2015). However, for humans CR is a difficult practice to maintain and may have pleiotropic effects depending on genetic constitution, environmental factors and stage of life. Likewise, the long-term use of rapamycin is limited by the risk of side effects, including disturbed glucose homeostasis, impaired would healing, gastrointestinal discomfort and others (Augustine, Bodziak, & Hricik, 2007; de Oliveira et al., 2011; Lamming et al., 2012; Wilkinson et al., 2012). Therefore, there is a need to investigate alternative targets that are part of the CR/mTORC1 pathway that can be manipulated to reach similar beneficial effects. Our work suggests that the transcription factor C/EBPβ may provide such a target.

C/EBPβ regulates the expression of metabolic genes in liver and adipose tissue (Desvergne, Michalik, & Wahli, 2006; Roesler, 2001). From its mRNA three protein isoforms are synthesized through the usage of different translation initiation sites: two isoforms acting as transcriptional activators, Liver Activator Protein (LAP) -1 and -2, and a transcriptional inhibitory isoform called Liver-enriched Inhibitory Protein (LIP) (Descombes & Schibler, 1991). We showed earlier that translation into LIP depends on a *cis*-regulatory uORF (**Figure 1A**) and is stimulated by mTORC1 signalling (Calkhoven, Muller, & Leutz, 2000; Jundt et al., 2005; Zidek et al., 2015). Pharmacological or CR-induced inhibition of mTORC1 in mice selectively reduces LIP-protein synthesis and thereby increases the LAP/LIP ratio in different tissues, which is associated with metabolic improvements resembling CR (Albert & Hall, 2015; Zidek et al., 2015). Recently we have developed a screening strategy for the discovery of small molecule drugs that suppress LIP expression, demonstrating that LIP expression is therapeutically targetable (Zaini et al., 2017).

Results and discussion

Others showed that LIP levels increase during aging in liver and white adipose tissue (WAT) (Hsieh et al., 1998; Karagiannides et al., 2001; Timchenko et al., 2006). Similarly, in our cohorts of wt C57BL/6 mice LIP levels are significantly higher in livers of old (20-22 months) versus young (5 months) mice, resulting in a decrease in LAP/LIP ratios during ageing (**Figure 1B, C - figure supplement 1**). In contrast, in C/EBPβ$^{\Delta uORF}$ mice LIP levels are low and stay low in old mice. LAP levels in C/EBPβ$^{\Delta uORF}$ males and to a lesser extend in females are increased, which is probably due to additional initiation events at the LAP-AUG by ribosomes that normally would have initiated at the uORF (Calkhoven et al., 2000). The C/EBPβ-mRNA levels are comparable at different ages and in the different genotypes (**Figure 1D and E**). Thus, LIP levels increase with age and this increase is dependent on the uORF in the C/EBPβ-mRNA.

We hypothesised that the C/EBPβ$^{\Delta uORF}$ mutation may have positive effects on healthspan and lifespan based on the CR-like metabolic improvements in C/EBPβ$^{\Delta uORF}$ mice, including enhanced fatty acid oxidation and lack of steatosis, improved insulin sensitivity and

glucose tolerance and higher adiponectin levels (Zidek et al., 2015). A lifespan experiment was set up comparing C/EBPβ$^{\Delta uORF}$ mice with wt littermates (C57BL/6) in cohorts of 50 mice of each genotype and gender. The survival curves revealed an increase in median survival of 20.6% (difference in overall survival p=0.0014 log-rank test, n=50) for the female C/EBPβ$^{\Delta uORF}$ mice compared to wt littermates (**Figure 2A**). From the 10% longest-lived females, nine out of ten were C/EBPβ$^{\Delta uORF}$ mice (**Table supplement 1**), showing that the maximum lifespan of C/EBPβ$^{\Delta uORF}$ females is significantly increased (p=0.0157 Fisher's exact test). If maximum lifespan is determined by the mean survival of the longest-lived 10% of each cohort, C/EBPβ$^{\Delta uORF}$ females show an increase of 9.14% (p-value=0.00105 Student's t-test.). For the male cohort we observed a modest increase in median survival of 5.2%, however the overall survival was not significantly increased (p=0.4647 log-rank test, n=50) (**Figure 2B**). The increase in median survival of the combined cohort of C/EBPβ$^{\Delta uORF}$ mice (males & females) was 10.5% (with a significant increase in overall survival p=0.0323 log-rank test, n=100) (**Figure supplement 2 and table supplement 1**). The observed median survival for wt females (623 days) is lower than what most other labs have reported for C57BL/6 females. We reasoned that this was due to a high incidence of ulcerative dermatitis (UD) we observed particularly in our female cohort (females: 19 mice or 38% for wt and 26 mice or 52% for C/EBPβ$^{\Delta uORF}$; males: 15 mice or 30% for wt and 10 mice or 20% for C/EBPβ$^{\Delta uORF}$). UD is a common and spontaneous condition in mice with a C57BL/6 background that progress to a severity that euthanasia is inevitable (Hampton et al., 2012). Therefore, survival curves were also calculated separately for UD-free mice and for mice that were euthanized because of serious UD (**Figure 2 C-F** and **table supplement 1** for complete overview). These data show that median lifespan of UD-free wt females are in a more normal range (740 days) and that the C/EBPβ$^{\Delta uORF}$ mutation results in a significant increase of median survival specifically in females irrespective of the condition of UD. Moreover, the median survival of the C/EBPβ$^{\Delta uORF}$ UD-free females (860.5 days) is higher compared to both wt females and wt males (829 days). The separate analysis of males with or without UD in both cases didn't show any significant difference in lifespan (**Figure 2D and F** - **figure supplement 2B and C**) similarly to the analysis of the whole cohort indicating that the C/EBPβ$^{\Delta uORF}$ mutation increases lifespan specifically in females.

Similar to our study several other studies report on sex specific differences in lifespan regulation. Calorie restriction by 20% has a greater lifespan extending effect in female C57BL/6 or DBA/2J mice compared to males (Mitchell et al., 2016). In addition, prolonged treatment with the mTORC1-inhibitor rapamycin starting from midlife has lifespan extending effects that are much stronger in females than in males using genetically heterogeneous mice as well as C57BL/6 mice (Fok et al., 2014; Harrison et al., 2009; Miller et al., 2011; Y. Zhang et al., 2014). On the contrary, transient rapamycin treatment for 90 days during midlife induces extension of lifespan in males but not in females depending on the dose (Bitto et al., 2016). Moderate overexpression of the mTORC1-inhibitor TSC1 or deletion of the ribosomal S6 protein kinase 1 (S6K1), downstream of mTORC1, result in lifespan extension only in females (Selman et al., 2009; H. M. Zhang, Diaz, Walsh, & Zhang, 2017). Mutations affecting both mTORC1 and mTORC2 show ambiguous effects; lifespan extension was limited to females in mice heterozygous for mTOR and its cofactor mammalian lethal with Sec 13 protein 8 (mLST8) (Lamming et al., 2012), while in a mTOR-hypomorphic mouse model lifespan is extended in both males and females (Wu et al., 2013). Notably, the reduction of LIP expression under low mTORC1 signalling is dependent on 4E-BP1/2 function and not on inhibition of S6K1 (Zidek et al., 2015). Thus, the bias towards female lifespan extension upon reduced mTORC1 signalling seems to be a common feature irrespective of whether the S6K1 or 4E-BP branch is affected. Also in mouse strains with alterations in other pathways like the somatotropic axis lifespan extension is often, but not always, more pronounced in females (Brown-Borg, 2009). Examples of somatotropic-related female biased lifespan extension are Ames dwarf mice that are deficient in growth hormone (GH) and prolactin production (Brown-Borg, Borg, Meliska, & Bartke, 1996) and insulin-like growth factor 1 (IGF-1) receptor heterozygous mice The reason for the mostly female biased lifespan extension upon inhibition of mTORC1 signalling or in the other mentioned mouse models is not known.

Aging is the most important risk factor for development of cancer. A reduction in cancer incidence is recurrently observed upon CR, rapamycin-treatment or manipulation of other pathways that increase longevity in several animal models (Anisimov et al., 2011; Colman et al., 2009; Komarova et al., 2012; Mattison et al., 2012; Neff et al., 2013; Serrano, 2016; Weindruch & Walford, 1982). Mice in the lifespan cohorts that died or were sacrificed

according to humane endpoint criteria underwent necropsy and tumours were analysed by a board certified veterinary pathologists of the Dutch Molecular Pathology Centre (DMPC). The incidence of neoplasms was markedly reduced in female C/EBPβ$^{\Delta uORF}$ mice compared to female wt mice (68% -> 45,8%, p=0.025 Fisher's exact test) (**Figure 3A**). Furthermore, tumours were detected on necropsy at a higher age in female C/EBPβ$^{\Delta uORF}$ mice compared to wt mice indicating a delay in tumour development (**Figure 3B**). The increase in median survival of the tumour bearing C/EBPβ$^{\Delta uORF}$ females was 25.49% compared to that of tumour bearing wt females (p=0.0217 log-rank test) (**Figure supplement 3A**). Also the tumour load (number of different tumour types per mouse) and the tumour spread (total number of differently located tumours per mouse irrespective of the tumour type) were lower in female C/EBPβ$^{\Delta uORF}$ mice (**Figure supplement 3B**). For males no significant reduction in tumour incidence was detected in C/EBPβ$^{\Delta uORF}$ mice (**Figure 3C and 3D**). The survival of tumour bearing mice and the tumour load was similar in wt and C/EBPβ$^{\Delta uORF}$ males, while the tumour spread seems to be even slightly increased in C/EBPβ$^{\Delta uORF}$ male mice (**Figure supplement 3C, D**). The main tumour types found in female mice were lymphoma, hepatocellular carcinoma and histiocytic sarcoma. The occurrence of all three types was reduced in C/EBPβ$^{\Delta uORF}$ females (**Table supplement 2**). For other tumour types the single numbers are too small to make a clear statement about a change in frequency. In male mice hepatocellular carcinoma and histiocytic sarcoma were the most frequent tumour types observed. Although the overall tumour incidence was similar in C/EBPβ$^{\Delta uORF}$ and wt males, the frequency of hepatocellular carcinoma was reduced in the C/EBPβ$^{\Delta uORF}$ males (**Table supplement 2**). Notably, knockin mice with elevated LIP levels show an increased tumour incidence upon ageing that goes along with reduced survival compared to wt controls (Begay et al., 2015). LIP overexpression can stimulate tumour cell proliferation, migration and transformation in vitro and high LIP levels have been detected in different human tumour tissues (Anand et al., 2014; Arnal-Estape et al., 2010; Calkhoven et al., 2000; Haas et al., 2010; Jundt et al., 2005; Park et al., 2013; Raught et al., 1996; Zahnow, Younes, Laucirica, & Rosen, 1997). Taken together the studies support an oncogenic role of LIP in tumour development and suggest that the reduction of LIP in the C/EBPβ$^{\Delta uORF}$ mice counteracts tumour development at least partially by cell intrinsic mechanisms.

Apart from the reduced tumour incidence and the increase in survival of tumour-bearing C/EBPβ$^{\Delta uORF}$ females, also the survival of tumour-free female C/EBPβ$^{\Delta uORF}$ mice was significantly extended by 25.13% (p=0.0467 log-rank test) compared to wt tumour-free females (**Figure supplement 3E**). This suggests that both the tumour incidence and additional unrelated factors contribute to the increased survival of C/EBPβ$^{\Delta uORF}$ females. The observed increase in median lifespan of tumour-free C/EBPβ$^{\Delta uORF}$ males of 19.71% does not correlate with a statistically significant increase in the overall survival (p=0.4647 log-rank test) (**Figure supplement 3F**). However, the survival curve points to a possible health improvement in the median phase of the male lifespan. Taken together, the C/EBPβ$^{\Delta uORF}$ mutation in mice restricting the expression of LIP results in a significant lifespan extension and decreased tumour incidence in females but not in males.

Typically, CR-mediated, genetic or pharmacological suppression of mTORC1 signalling is accompanied by the attenuation of an age-associated decline of health parameters (Johnson, Rabinovitch, & Kaeberlein, 2013). We examined the selected health parameters of body weight and composition, glucose tolerance, naïve/memory T-cell ratio, motor coordination and muscle strength in separate ageing cohorts of young (3-5 months) and old (18-20 months for females and 20-22 months for males) mice. In addition, we compared the histological appearance of selected tissues (liver, muscle, pancreas, skin, spleen and bone) between old (20/22 months) wt and C/EBPβ$^{\Delta uORF}$ mice. Body weight was significantly increased in all old mice (**Figure 4A, B**). The increase for the old female C/EBPβ$^{\Delta uORF}$ mice was significantly smaller compared to old wt littermates, while for the males there was no significant difference between the genotypes (**Figure 4A, B**). The slightly lower body weight for the young C/EBPβ$^{\Delta uORF}$ males was also observed in our previous study (Zidek et al., 2015). A similar pattern was observed regarding the fat content that was measured by abdominal computed tomography (CT) analysis (**Figure 4C, D**). The volumes of total fat increased strongly in old mice both in visceral and subcutaneous fat depots (**Figure supplement 4A, B**). Old female C/EBPβ$^{\Delta uORF}$ mice accumulated significantly less fat in the visceral and subcutaneous fat depots than wt females, while there was no difference for male mice (**Figure supplement 4A, B**). The lean body mass was slightly lower in old female C/EBPβ$^{\Delta uORF}$ mice and increased in male wt mice compared to young mice (**Figure**

supplement 4A, B). Thus, female C/EBPβ$^{\Delta uORF}$ mice gain less fat upon aging similar to mice under CR or upon prolonged rapamycin treatment (Fang et al., 2013) (**Figure supplement 4C**), which probably contributes to an improved health state upon aging and to the extension in lifespan. In contrast, although male C/EBPβ$^{\Delta uORF}$ mice had a lower body weight and subcutaneous fat content at a young age compared to wt mice they were not able to maintain this difference during the aging process, which correlates with the lack in lifespan extension. In addition, we found an increase in mRNA expression of the macrophage marker CD68 as a measure for age-related macrophage infiltration in visceral WAT of old mice, which was attenuated in female C/EBPβ$^{\Delta uORF}$ mice but not in male C/EBPβ$^{\Delta uORF}$ mice (**Figure supplement 4D**).

Impaired glucose tolerance is a hallmark of the aging process, which is improved by CR (Barzilai, Banerjee, Hawkins, Chen, & Rossetti, 1998; Mitchell et al., 2016). The intraperitoneal glucose tolerance test (IPGTT) showed that glucose clearance, calculated as the area under the curve (AUC), is significantly less efficient in old wt compared to young wt mice (**Figure 4E, F**). Old C/EBPβ$^{\Delta uORF}$ females and males perform significantly better in the IPGTT test than old wt littermates, which is reflected by the lower AUC value. Therefore, the C/EBPβ$^{\Delta uORF}$ mutation protects against age-related decline of glucose homeostasis in males and females.

The ageing associated increase in memory/naïve T-cell ratio is a robust indicator for the progression of the immunological ageing progress. At a young age naïve T cells predominate and memory T cells are relatively scarce. Upon ageing the naïve T cell population is strongly reduced with a concomitant increase in the memory T cell population, resulting in an increased ratio of memory to naïve T cells (Hakim, Flomerfelt, Boyiadzis, & Gress, 2004). The ratio of memory (CD44high) to naïve (CD44low/CD62Lhigh) cytotoxic T (CD8+) cells or memory (CD44high) to naïve (CD44low/CD62Lhigh) helper T (CD4+) cells was analysed by flow cytometric analysis. Both increased upon aging in the blood of males and females of both genotypes (**Figure 5A-D**). However in C/EBPβ$^{\Delta uORF}$ mice of both genders this increase was significantly attenuated compared to wt mice (**Figure 5A-D - figure supplement 5A-D**). These data suggest that the C/EBPβ$^{\Delta uORF}$ mutation preserves a more juvenile immunological phenotype during ageing.

Aging is associated with a significant decline in motor coordination and muscle strength (Barreto, Huang, & Giffard, 2010; Demontis, Piccirillo, Goldberg, & Perrimon, 2013). In the rotarod test the time is measured that mice endure on a turning and accelerating rod as an indication for their motor-coordination. As expected, rotarod performance decreased with age both for wt female and male mice (**Figure 6A**). Remarkably, rotarod performance was completely preserved in old C/EBPβ$^{\Delta uORF}$ females but not in C/EBPβ$^{\Delta uORF}$ males. In the beam walking test the required crossing time and number of paw slips of mice traversing a narrow beam are measured. Old mice needed more time to cross the beam reflecting loss of motor coordination upon ageing (**Figure 6B**). The aging-associated increase of the crossing time was less severe in C/EBPβ$^{\Delta uORF}$ males and females, although statistically significant only in males (**Figure 6B**). Nevertheless, the strong increase in the number of paw slips in old wt mice is almost completely attenuated in C/EBPβ$^{\Delta uORF}$ males and females (**Figure 6C**). Note that the number of paw slips by young C/EBPβ$^{\Delta uORF}$ males is already significantly lower compared to young wt males. During the wire hang test the time is measured that mice endure to hang from an elevated wire which serves as an indication for limb skeletal muscle strength (Brooks & Dunnett, 2009). Similar to the rotarod test, the decline in wire hang performance that is seen in old wt mice is completely restored for the female but not for the male C/EBPβ$^{\Delta uORF}$ mice (**Figure 6D**).

Taken together these data demonstrate that the decline in motor coordination and muscle strength is less severe and partly abrogated in female C/EBPβ$^{\Delta uORF}$ mice. The results for the old male C/EBPβ$^{\Delta uORF}$ mice are not that clear since they show an improved performance only in the beam walking test. One possible explanation is that only the beam walking test measures purely motor coordination skills whereas the results from the rotarod and wire hang tests are influenced in addition by muscle strength and endurance. Old C/EBPβ$^{\Delta uORF}$ males thus might have maintained their motor coordination upon ageing but still suffer from an ageing-dependent loss of muscle strength.

By histological examination of different tissues we observed a reduction in some age-related alterations in C/EBPβ$^{\Delta uORF}$ mice compared to old wt controls (**Table supplement 3**). We observed a reduced severity of hepatocellular vacuolation and cytoplasmic nuclear inclusions in male C/EBPβ$^{\Delta uORF}$ mice; in the pancreas both male and female C/EBPβ$^{\Delta uORF}$

mice showed a reduced occurrence and severity of islet cell hyperplasia; in skeletal muscle the number of regenerating muscle fibres was higher in male C/EBPβ$^{\Delta uORF}$ mice; the incidence of dermal inflammation was lower in female C/EBPβ$^{\Delta uORF}$ mice. Unexpectedly, a slightly increased level of inflammation was detected in the livers of female C/EBPβ$^{\Delta uORF}$ mice; a condition believed to be detrimental for glucose homeostasis. However, recently this view was challenged by showing that hepatic inflammation, involving the activation of IKKβ, is beneficial for maintaining glucose homeostasis (Liu et al., 2016). The incidence of other potential age-related pathologies like focal acinar cell atrophy and inflammation in the pancreas, liver polyploidy, spleen lymphoid hyperplasia and extramedulary haematopoiesis, intramuscular adipose tissue infiltration, subcutaneous fat atrophy and bone density were not significantly altered between old wt and C/EBPβ$^{\Delta uORF}$ mice. We found slightly reduced plasma IGF-1 levels in old C/EBPβ$^{\Delta uORF}$ females compared to old wt females (**Table supplement 3**). A reduction in circulating IGF-1 levels was also found in mice under CR and is believed to be an important mediator of health- and lifespan extending effects of CR (Breese, Ingram, & Sonntag, 1991; Mitchell et al., 2016). Taken together our data show that multiple, but not all, ageing associated alterations are attenuated in C/EBPβ$^{\Delta uORF}$ mice, particularly in females.

Finally, we performed a comparative transcriptome analysis from livers of 5 and 20 months old wt and C/EBPβ$^{\Delta uORF}$ female mice (Müller, 2018). A principal component analysis revealed that there was a clear effect of the genotype on gene expression only in the old mice suggesting that the differences in gene expression between wt and C/EBPβ$^{\Delta uORF}$ mice are aging dependent (**Figure supplement 6**). This is supported by the finding that in young mice only 42 genes were differentially regulated between wt and C/EBPβ$^{\Delta uORF}$ mice (FDR < 0.01; 24 genes upregulated and 18 genes down-regulated in C/EBPβ$^{\Delta uORF}$ mice compared to wt mice) while in old mice we found 152 differentially regulated genes (FDR < 0.01; 127 genes upregulated and 25 genes downregulated in C/EBPβ$^{\Delta uORF}$ mice compared to wt mice). Gene ontology (GO) analysis using the David database (Huang da, Sherman, & Lempicki, 2009) of the genes upregulated in old C/EBPβ$^{\Delta uORF}$ mice in comparison to old wt mice revealed GO terms including “External side of plasma membrane”, “Positive regulation of T-cell proliferation”, and “immune response” (see **Table supplement 4** for the complete list of GO-terms) whereas the GO-terms: “Acute phase” and “Extracellular space” were significantly

295 downregulated (**Table supplement 5**). Acute phase response genes are associated with
296 inflammation and their expression in the liver increases upon ageing (Lee et al., 2012). Like in
297 old C/EBPβ$^{\Delta uORF}$ mice expression of acute phase response genes is also inhibited by caloric
298 restriction or treatment with the CR mimetic metformin (Martin-Montalvo et al., 2013)
299 suggesting similar protective mechanisms. The fact that we see the up-regulation of several
300 GO-terms connected to lymphocyte biology fits to the increase in lymphoplasmatic
301 inflammation in the liver of old female C/EBPβ$^{\Delta uORF}$ mice observed by pathological analysis
302 (**Table supplement 3**). Although it is generally believed that ageing associated lymphocyte
303 infiltration rather promotes the ageing process by increasing inflammatory signals (Singh et
304 al., 2008), it could also contribute to the removal of senescent or pro-tumorigenic cells,
305 thereby acting protective (Kang et al., 2011). Despite the improved metabolic phenotype of
306 C/EBPβ$^{\Delta uORF}$ mice (Zidek et al., 2015), the analysis did not reveal GO-terms related to
307 metabolism. We reasoned that metabolic genes might not be detected as differentially
308 regulated because they are subject of expression heterogeneity in old mice. Comparison
309 between the coefficient of variation of individual transcripts between young and old mice
310 revealed that inter-individual variation of gene expression increases with age in both
311 genotypes (**Figure 7A, B**) supporting earlier observations made by others (White et al.,
312 2015). Direct comparison between old wt and C/EBPβ$^{\Delta uORF}$ mice showed that this effect is
313 less pronounced in C/EBPβ$^{\Delta uORF}$ mice (**Figure 7C**). KEGG (Kyoto Encyclopedia of Genes and
314 Genomes) pathway and GO-term enrichment analysis of the highly variably expressed genes
315 in the aged livers revealed that in wt mice particularly metabolic genes related to fatty acid
316 metabolism and oxidative phosphorylation were affected which was not observed in
317 C/EBPβ$^{\Delta uORF}$ mice (**Figure 7D - table supplement 6 and 7**). On the other hand genes
318 involved in cell cycle, transcription and RNA biology showed higher inter-individual variation in
319 old C/EBPβ$^{\Delta uORF}$ mice compared to wt controls (**Table supplement 7**). These findings
320 suggest that expression control of metabolic genes stays more robust upon aging in
321 C/EBPβ$^{\Delta uORF}$ mice. Whether the increased inter-individual variation of metabolic transcripts in
322 old wt mice is a direct effect of the observed increase of the inhibitory-acting LIP isoform or is
323 due to unknown secondary effects has to be clarified in future studies. It is however
324 conceivable that increased transcriptional robustness in the old C/EBPβ$^{\Delta uORF}$ mice contributes

to the extension in health- and lifespan of the female C/EBPβ$^{\Delta uORF}$ mice. This idea is supported by our finding that also genes involved in ageing-associated diseases like Non-alcoholic fatty liver disease, Alzheimer's disease, Parkinson's disease, Huntington's disease and cancer (Chemical carcinogenesis) are affected by high inter-individual variation in expression levels in wt but not in C/EBPβ$^{\Delta uORF}$ mice (**Figure 7D**).

In summary, reduced signalling through the mTORC1 pathway is thought to mediate many of the beneficial effects of CR or rapamycin treatment (Johnson et al., 2013), and both conditions restrict mTORC1-controlled translation into LIP (Calkhoven et al., 2000; Zidek et al., 2015). These and other studies firmly place LIP function downstream of mTORC1 at the nexus of nutrient signalling and metabolic gene regulation. However, upon ageing, LIP expression increases (the LAP/LIP ratio decreases) in the liver whereas no significant changes in mTORC1 were detected (**Figure supplement 7**). Possibly, other pathways play a role in age-related upregulation of LIP as has been described for CUGBP1 (Karagiannides et al., 2001; Timchenko et al., 2006).

Experimental reduction of the transcription factor C/EBPβ-LIP in mice recapitulates many of the effects of CR or treatment with rapamycin, including the reduced cancer incidence and the generally more pronounced extension of lifespan in females (**Figure 8**). We have developed a high-throughput screening screening strategy that allows for discovery of small molecular compounds that suppress the translation into LIP (Zaini et al., 2017). The identification of such compounds or conditions that reduce LIP translation may reveal new ways of CR-mimetic based therapeutic strategies beyond those using mTORC1 inhibition.

Material and methods

Mice

C/EBPβ$^{\Delta uORF}$ mice described in (Wethmar et al., 2010) were back-crossed for 12 generations into the C57BL/6J genetic background. Mice were kept at a standard 12-h light/dark cycle at 22ºC in individually ventilated cages (IVC) in a specific-pathogen-free (SPF) animal facility on a standard mouse diet (Harlan Teklad 2916). Mice of the ageing cohort were analysed between 3 and 5 months of age (young) and between 18 and 20 months (old females) or

between 20 and 22 months (old males) and were derived from the same breeding pairs as mice used in the lifespan experiment. The body weight of the ageing cohorts was determined before the start of the experimental analysis. All of the animals were handled according to approved institutional animal care and use committee (IACUC) protocols of the Thüringer Landesamt für Verbraucherschutz (#03-005/13) and University of Groningen (#6996A).

Lifespan experiment

C/EBPβ$^{\Delta uORF}$ and wt littermates (50 mice from each genotype and gender) derived from mating between heterozygous males and females were subjected to a lifespan experiment. Mice were housed in groups with maximum five female mice or four male mice per cage (separated in genotypes and genders) and did not participate in other experiments. Mice were checked daily and the lifespan of every mouse (days) was recorded. Mice were euthanized when the condition of the animal was judged as moribund and/or to be incompatible with continued survival due to severe discomfort based on the independent assessment of experienced animal caretakers. All mice that were found dead or were euthanized underwent necropsy with a few exceptions when the grade of decomposition of dead animals prevented further examination (number of mice without necropsy: n=0 for wt females; n=2 for C/EBPβ$^{\Delta uORF}$ females; n=3 for wt males and n=5 for C/EBPβ$^{\Delta uORF}$ males. Survival curves were calculated with the Kaplan-Meier method. Statistical significance was determined by the log-rank test using GraphPath Prism 6 software. Maximum lifespan was determined by the number of mice for each genotype that were within the 10% longest-lived mice of the combined (wt and C C/EBPβ$^{\Delta uORF}$) cohorts. Statistical significance of observed differences was calculated with Fisher's exact test. In addition, the mean lifespan (±SEM) of the 10% longest lived mice within one genotype was compared to the mean lifespan of the 10% longest lived mice of the other genotype, and the statistical significance was calculated with the Student's T-test.

Tumour incidence

Suspected tumour tissue found during necropsy of the lifespan cohorts was fixed in 4% paraformaldehyde and Haematoxylin & Eosin stained tissue slices were analysed by

385 experienced board-certified veterinary pathologists of the Dutch Molecular Pathology Centre
386 (Utrecht University) to diagnose the tumour type. Tumour incidence was calculated as
387 percentage of mice with pathologically confirmed tumours in respect to all mice from the same
388 cohort that underwent necropsy. Tumour occurrence was defined as the time of death of an
389 animal in which a pathologically confirmed tumour was found. Tumour load was defined as
390 number of different tumour types found in the same mouse and tumour spread was defined
391 as number of different organs harbouring a tumour within the same mouse irrespective of the
392 tumour type with the exception that in those cases in which different tumour types were found
393 in the same organ a number >1 was rated.
394
395 **Motor coordination experiments**
396 Rotarod test: Mice were habituated to the test situation by placing them on a rotarod (Ugo
397 Basile) with constant rotation (5 rpm) for 5 min at two consecutive days with two trials per
398 mouse per day separated by an interval of 30 min. In the test phase two trials per mouse
399 were performed with accelerating rotation (2-50 rpm within 4 min) with a maximum trial
400 duration of 5 min in which the time was measured until mice fell off the rod. Beam walking
401 test: Mice were trained by using a beam of 3 cm width and 100 cm in length at two
402 consecutive days (one trial per mouse per day). At the test day mice had to pass a 1 cm wide
403 beam, 100 cm in length and beam crossing time and number off paw slips upon crossing was
404 measured during 3 trials per mouse that were separated by an interval of 20 min. To
405 determine of the number of mistakes the number of paw slips per trial was counted upon
406 examination of recorded videos. Wire Hang test: To measure limb grip strength mice were
407 placed with their four limbs at a grid with wire diameter of 1 mm at 20 cm over the layer of
408 bedding material and the hanging time was measured until mice loosened their grip and fell
409 down. Three trials of maximal 60s per mouse were performed that were separated by an
410 interval of 30 min.
411
412 **Body composition**

The body composition was measured using an Aloka LaTheta Laboratory Computed Tomograph LCT-100A (Zinsser Analytic) as described in (Zidek et al., 2015). Percentage body fat was calculated in relation to the sum of lean mass and fat mass.

Bone measurements

Bones of the hind legs were freed from soft tissue and fixed in 4% paraformaldehyde. For determination of the bone volume, trabecular thickness, trabecular number and trabecular separation femurs were analysed by micro CT (Skyscan 1176, Bruker) equipped with an X-ray tube (50 kV/500 mA). The resolution was 9 mm, rotation step was set at 1ºC, and a 0.5 mm aluminium filter was used. For reconstruction of femora, the region of interest was defined 0.45 mm (for trabecular bone) or 4.05 mm (for cortical bone) apart from the distal growth plate into the diaphysis spanning 2.7 mm (for trabecular bone) or 1.8 mm (for cortical bone). Trabecular bone volume/tissue volume (%), trabecular number per µm, trabecular thickness (mm) and trabecular separation (intertrabecular distance, mm) was determined according to guidelines by ASBMR Histomorphometry Nomenclature Committee (Dempster et al., 2013).

Glucose tolerance

The intraperitoneal (i.p.) glucose tolerance test (IPGTT) was performed as described in (Zidek et al., 2015). Mice without initial increase in blood glucose concentration were excluded from the analysis.

Flow cytometry

Blood cells from 300 µl blood were incubated in RBC-Lysis buffer (Biolegend) to lyse the red blood cells. Remaining cells were washed and incubated with a cocktail of fluorochrome-conjugated antibodies (CD4-PE-Cy7 (#552775) and CD62L-FITC (#561917) from BD Pharmingen; CD3e-PE (#12-0031), CD8a-eFluor 450 (#48-0081) and CD44-APC (#17-0441) from eBioscience.), incubated with propidium iodide for the detection of dead cells and analysed using the FACSCanto II analyser (BD Biosciences). The following T cell subsets were quantified: $CD3^+$, $CD8^+$, $CD44^{high}$ cytotoxic memory T cells; $CD3^+$, $CD8^+$, $CD44^{low}$,

443 CD62L^{high} cytotoxic naïve T cells, CD3^{+}, CD4^{+}, CD44^{high} helper memory T cells and CD3^{+},
444 CD4^{+}, CD44^{low}, CD62L^{high} helper naïve T cells.
445
446 **Histology**
447 Tissue pieces were fixed with 4% paraformaldehyde and embedded in paraffin. Sections were
448 stained with Haematoxylin and Eosin (H&E) and age-related pathologies or tumour types
449 were analysed by experienced board-certified veterinary pathologists of the Dutch Molecular
450 Pathology Centre (Utrecht University). Semi-quantification of muscle regeneration was done
451 by counting the number of myofibers with a row of internalized nuclei (>4) for five 200x fields.
452 Other ageing-associated lesions were scored subjectively and the severity of the lesions was
453 graded on a scale between 0 and 3 with 0 = absent; 1 = mild; 2 = moderate and 3 = severe.
454
455 **Immunoblotting and quantification**
456 Mouse liver tissue was homogenized on ice with a glass douncer in RIPA buffer (150 mM
457 NaCl, 1% NP40, 0.5% sodium deoxycholate, 0.1% SDS, 50 mM TRIS pH 8.0 supplemented
458 with protease and phosphatase inhibitors) and sonicated. Equal amounts of total protein were
459 separated by SDS-PAGE, transferred to a PVDF membrane and incubated with the following
460 antibodies: C/EBPβ (E299) and β-actin (ab16039) from Abcam; 4E-BP1 (C-19) from Santa
461 Cruz; phospho-p70S6K (Thr389) (108D2), p70S6K (#9202) and phospho-4E-BP1 (Thr 37/46)
462 (#9459) from Cell Signaling Technology and HRP-linked anti rabbit IgG from GE Healthcare.
463 Lightning Plus ECL reagent (Perkin Elmer) was used for detection and for re-probing
464 membranes were incubated in Restore Western Blot Stripping buffer (Perbio). The detection
465 and quantification of protein bands was performed with the Image Quant LAS 4000 Mini
466 Imager (GE Healthcare) using the supplied software.
467
468 **Quantitative real-time PCR**
469 Mouse liver or visceral fat tissue was homogenized on ice with a motor driven pellet pestle
470 (Kontes) in the presence of QIAzol reagent (QIAGEN) and total RNA was isolated as
471 described in(Zidek et al., 2015). cDNA synthesis was performed from 1 µg of total RNA with
472 the Transcriptor First Strand cDNA Synthesis Kit (Roche) using random hexamer primers.

qRT-was performed with the LightCycler 480 SYBR Green I Master mix (Roche) using the following primers: β-actin: 5'-AGA GGG AAA TCG TGC GTG AC-3' and 5'-CAA TAG TGA TGA CCT GGC CGT-3'; C/EBPβ: 5'-CTG CGG GGT TGT TGA TGT-3' and 5'-ATG CTC GAA ACG GAA AAG GT-3'; CD68: 5'-GCC CAC CAC CAC CAG TCA CG-3' and 5'- GTG GTC CAG GGT GAG GGC CA-3'.

Enzyme-linked immune-sorbent assay (ELISA)

Plasma was prepared as described in (Zidek et al., 2015) and the IGF-1 specific ELISA was performed according to the instructions of the manufacturer (BioCat).

RNA-seq Analysis

Liver tissue from young (5 months) and old (20 months) wt and C/EBPβ$^{\Delta uORF}$ mice (from six individuals per group) was homogenized on ice with a motor driven pellet pestle (Kontes) in the presence of QIAzol reagent (Qiagen) and total RNA was isolated as described in Zidek et al(Zidek et al., 2015). Preparation of the sequencing libraries was performed using the TruSeq Sample Preparation V2 Kit (Illumina) according to the manufacturer's instructions. High-throughput single-end sequencing (65 bp) of the libraries was performed with an Illumina HiSeq 2500 instrument. Reads were aligned and quantified using STAR 2.5.2b(Dobin et al., 2013) against primary assembly GRCm38 using Ensembl gene build 86 (http://www.ensembl.org). Genes with average expression level below 1 fragment per million (FPM) were excluded from the analysis. A generalized linear model was used to identify differential gene expression using EdgeR package (McCarthy, Roche, & Forde, 2012; Robinson, McCarthy, & Smyth, 2010). The library normalization was left at the standard setting (trimmed mean of M-values, TMM). The resulting p-values were corrected for multiple testing using the Benjamini-Hochberg procedure. Data visualization, calculation of CV (coefficient of variation) and statistical tests were conducted using custom R scripts (de Jong, 2018). Gene ontology (GO) analysis was performed using the DAVID database version 6.8 (Huang da et al., 2009) with default DAVID database setting with medium stringency and *Mus musculus* background. KEGG pathway analysis was performed using gProfiler tool (Reimand et al., 2016). For dataset see (Müller, 2018).

503

504 **Statistical analysis**

505 Biological replication is indicated (n=x). All graphs show average ± standard error of the mean
506 (s.e.m.). The unpaired, two-tailed Student's t-Test was used to calculate statistical
507 significance of results with * p< 0.05; ** p<0.01; *** p< 0.001. Significance of the differences in
508 survival curves were analysed using the log-rank test and significance of the difference in
509 maximum lifespan (number of mice from one cohort within the 10% longest lived mice
510 calculated from the combined cohort) and tumour incidence was calculated using the Fisher's
511 exact test with *p<0.05.

512

513

514 **Acknowledgements**

515 We thank Rafael de Cabo, NIA Baltimore for advice with the lifespan experiment. At the
516 ERIBA/UMCG Groningen we thank Mirjam Koster for technical assistance with histology and
517 Gerald de Haan for critical reading of the manuscript. At the FLI we thank we thank Sabrina
518 Eichwald for technical assistance, Lucien Frappart and Dominique Galendo for advice on
519 necropsy, the staff of the animal house facility in particular Anja Baar and Juliane Brüchert for
520 massive support with the lifespan experiment, Nico Andreas for advice concerning the flow
521 cytometry experiments, Anne Gompf for technical assistance with flow cytometry, Maik
522 Baldauf for paraffin embedding and Christina Valkova for advice with the motor coordination
523 experiments. L.M.Z was supported by the Deutsche Forschungsgemeinschaft (DFG) through
524 a grant to C.F.C. (CA 283/1-1) and a grant to J.V.M. (MA-3975/2-1). T.A. was supported by
525 the Leibniz Graduate School on Ageing and Age-Related Diseases (LGSA; www.fli-
526 leibniz.de/phd/) P.L. was supported by the Collaborative Research Centre 1149 'Trauma'
527 (INST 40/492-1) and DFG priority program Immunobone (Tu220/6) to a grant to J.P.T.

528

529

530 **Author contributions**

531 C.M., M.Z, T.A, P.L, V.K, M.A.Z, G.K, and J.M. performed experiments; L.H, A.de B.
532 performed patho-histological analysis; T.de J, V.G. performed bioinformatic analysis; J.P.T,

D.V, J.von M. and Z-Q. W. designed and advised on animal experiments. C.M., L.M.Z., J. von M., V.G., Z-Q. W and C.F.C wrote the manuscript. C.F.C supervised the project.

Competing financial interests

No competing financial interest

References

Albert, V., & Hall, M. N. (2015). Reduced C/EBPbeta-LIP translation improves metabolic health. *EMBO Rep, 16*(8), 881-882. doi:10.15252/embr.201540757

Anand, S., Ebner, J., Warren, C. B., Raam, M. S., Piliang, M., Billings, S. D., & Maytin, E. V. (2014). C/EBP transcription factors in human squamous cell carcinoma: selective changes in expression of isoforms correlate with the neoplastic state. *PLoS One, 9*(11), e112073. doi:10.1371/journal.pone.0112073

Anisimov, V. N., Zabezhinski, M. A., Popovich, I. G., Piskunova, T. S., Semenchenko, A. V., Tyndyk, M. L., . . . Blagosklonny, M. V. (2011). Rapamycin increases lifespan and inhibits spontaneous tumorigenesis in inbred female mice. *Cell Cycle, 10*(24), 4230-4236. doi:10.4161/cc.10.24.18486

Arnal-Estape, A., Tarragona, M., Morales, M., Guiu, M., Nadal, C., Massague, J., & Gomis, R. R. (2010). HER2 silences tumor suppression in breast cancer cells by switching expression of C/EBPss isoforms. *Cancer Res, 70*(23), 9927-9936. doi:10.1158/0008-5472.CAN-10-0869

Augustine, J. J., Bodziak, K. A., & Hricik, D. E. (2007). Use of sirolimus in solid organ transplantation. *Drugs, 67*(3), 369-391.

Barreto, G., Huang, T. T., & Giffard, R. G. (2010). Age-related defects in sensorimotor activity, spatial learning, and memory in C57BL/6 mice. *J Neurosurg Anesthesiol, 22*(3), 214-219. doi:10.1097/ANA.0b013e3181d56c98

Barzilai, N., Banerjee, S., Hawkins, M., Chen, W., & Rossetti, L. (1998). Caloric restriction reverses hepatic insulin resistance in aging rats by decreasing visceral fat. *J Clin Invest, 101*(7), 1353-1361. doi:10.1172/JCI485

Begay, V., Smink, J. J., Loddenkemper, C., Zimmermann, K., Rudolph, C., Scheller, M., . . . Leutz, A. (2015). Deregulation of the endogenous C/EBPbeta LIP isoform predisposes to tumorigenesis. *J Mol Med (Berl), 93*(1), 39-49. doi:10.1007/s00109-014-1215-5

Bitto, A., Ito, T. K., Pineda, V. V., LeTexier, N. J., Huang, H. Z., Sutlief, E., . . . Kaeberlein, M. (2016). Transient rapamycin treatment can increase lifespan and healthspan in middle-aged mice. *Elife, 5*. doi:10.7554/eLife.16351

Breese, C. R., Ingram, R. L., & Sonntag, W. E. (1991). Influence of age and long-term dietary restriction on plasma insulin-like growth factor-1 (IGF-1), IGF-1 gene expression, and IGF-1 binding proteins. *J Gerontol, 46*(5), B180-187.

584 Brooks, S. P., & Dunnett, S. B. (2009). Tests to assess motor phenotype in mice: a user's
585 guide. *Nat Rev Neurosci, 10*(7), 519-529. doi:10.1038/nrn2652
586
587 Brown-Borg, H. M. (2009). Hormonal control of aging in rodents: the somatotropic axis. *Mol*
588 *Cell Endocrinol, 299*(1), 64-71. doi:S0303-7207(08)00285-2 [pii]
589 10.1016/j.mce.2008.07.001
590
591 Brown-Borg, H. M., Borg, K. E., Meliska, C. J., & Bartke, A. (1996). Dwarf mice and the
592 ageing process. *Nature, 384*(6604), 33. doi:10.1038/384033a0
593
594 Calkhoven, C. F., Muller, C., & Leutz, A. (2000). Translational control of C/EBPalpha and
595 C/EBPbeta isoform expression. *Genes Dev, 14*(15), 1920-1932.
596
597 Colman, R. J., Anderson, R. M., Johnson, S. C., Kastman, E. K., Kosmatka, K. J., Beasley, T.
598 M., . . . Weindruch, R. (2009). Caloric restriction delays disease onset and mortality in
599 rhesus monkeys. *Science, 325*(5937), 201-204. doi:10.1126/science.1173635
600
601 de Jong, T. (2018). Processed data and R script for analysis and visualization of
602 transcriptome variability. Retrieved from
603 http://www.genomes.nl/CEBPB_delta_uORF/
604
605 de Oliveira, M. A., Martins, E. M. F., Wang, Q., Sonis, S., Demetri, G., George, S., . . .
606 Treister, N. S. (2011). Clinical presentation and management of mTOR inhibitor-
607 associated stomatitis. *Oral Oncol, 47*(10), 998-1003.
608 doi:10.1016/j.oraloncology.2011.08.009
609
610 Demontis, F., Piccirillo, R., Goldberg, A. L., & Perrimon, N. (2013). Mechanisms of skeletal
611 muscle aging: insights from Drosophila and mammalian models. *Dis Model Mech,*
612 *6*(6), 1339-1352. doi:10.1242/dmm.012559
613
614 Descombes, P., & Schibler, U. (1991). A liver-enriched transcriptional activator protein, LAP,
615 and a transcriptional inhibitory protein, LIP, are translated from the same mRNA. *Cell,*
616 *67*(3), 569-579. doi:0092-8674(91)90531-3 [pii]
617
618 Desvergne, B., Michalik, L., & Wahli, W. (2006). Transcriptional regulation of metabolism.
619 *Physiol Rev, 86*(2), 465-514. doi:10.1152/physrev.00025.2005
620
621 Dobin, A., Davis, C. A., Schlesinger, F., Drenkow, J., Zaleski, C., Jha, S., . . . Gingeras, T. R.
622 (2013). STAR: ultrafast universal RNA-seq aligner. *Bioinformatics, 29*(1), 15-21.
623 doi:10.1093/bioinformatics/bts635
624
625 Fang, Y., Westbrook, R., Hill, C., Boparai, R. K., Arum, O., Spong, A., . . . Bartke, A. (2013).
626 Duration of rapamycin treatment has differential effects on metabolism in mice. *Cell*
627 *Metab, 17*(3), 456-462. doi:10.1016/j.cmet.2013.02.008
628
629 Fok, W. C., Chen, Y., Bokov, A., Zhang, Y., Salmon, A. B., Diaz, V., . . . Richardson, A.
630 (2014). Mice fed rapamycin have an increase in lifespan associated with major
631 changes in the liver transcriptome. *PLoS One, 9*(1), e83988.
632 doi:10.1371/journal.pone.0083988
633
634 Haas, S. C., Huber, R., Gutsch, R., Kandemir, J. D., Cappello, C., Krauter, J., . . . Brand, K.
635 (2010). ITD- and FL-induced FLT3 signal transduction leads to increased C/EBPbeta-
636 LIP expression and LIP/LAP ratio by different signalling modules. *Br J Haematol,*
637 *148*(5), 777-790. doi:10.1111/j.1365-2141.2009.08012.x
638
639 Hakim, F. T., Flomerfelt, F. A., Boyiadzis, M., & Gress, R. E. (2004). Aging, immunity and
640 cancer. *Curr Opin Immunol, 16*(2), 151-156. doi:10.1016/j.coi.2004.01.009
641
642 Hampton, A. L., Hish, G. A., Aslam, M. N., Rothman, E. D., Bergin, I. L., Patterson, K. A., . . .
643 Rush, H. G. (2012). Progression of ulcerative dermatitis lesions in C57BL/6Crl mice

644 and the development of a scoring system for dermatitis lesions. *J Am Assoc Lab*
645 *Anim Sci, 51*(5), 586-593.
646
647 Harrison, D. E., Strong, R., Sharp, Z. D., Nelson, J. F., Astle, C. M., Flurkey, K., . . . Miller, R.
648 A. (2009). Rapamycin fed late in life extends lifespan in genetically heterogeneous
649 mice. *Nature, 460*(7253), 392-395. doi:10.1038/nature08221
650
651 Hsieh, C. C., Xiong, W., Xie, Q., Rabek, J. P., Scott, S. G., An, M. R., . . . Papaconstantinou,
652 J. (1998). Effects of age on the posttranscriptional regulation of CCAAT/enhancer
653 binding protein alpha and CCAAT/enhancer binding protein beta isoform synthesis in
654 control and LPS-treated livers. *Mol Biol Cell, 9*(6), 1479-1494.
655
656 Huang da, W., Sherman, B. T., & Lempicki, R. A. (2009). Systematic and integrative analysis
657 of large gene lists using DAVID bioinformatics resources. *Nat Protoc, 4*(1), 44-57.
658 doi:10.1038/nprot.2008.211
659
660 Johnson, S. C., Rabinovitch, P. S., & Kaeberlein, M. (2013). mTOR is a key modulator of
661 ageing and age-related disease. *Nature, 493*(7432), 338-345.
662 doi:10.1038/nature11861
663
664 Jundt, F., Raetzel, N., Muller, C., Calkhoven, C. F., Kley, K., Mathas, S., . . . Dorken, B.
665 (2005). A rapamycin derivative (everolimus) controls proliferation through down-
666 regulation of truncated CCAAT enhancer binding protein {beta} and NF-{kappa}B
667 activity in Hodgkin and anaplastic large cell lymphomas. *Blood, 106*(5), 1801-1807.
668 doi:2004-11-4513 [pii]
669 10.1182/blood-2004-11-4513
670
671 Kaeberlein, M., Rabinovitch, P. S., & Martin, G. M. (2015). Healthy aging: The ultimate
672 preventative medicine. *Science, 350*(6265), 1191-1193. doi:10.1126/science.aad3267
673
674 Kang, T. W., Yevsa, T., Woller, N., Hoenicke, L., Wuestefeld, T., Dauch, D., . . . Zender, L.
675 (2011). Senescence surveillance of pre-malignant hepatocytes limits liver cancer
676 development. *Nature, 479*(7374), 547-551. doi:10.1038/nature10599
677
678 Karagiannides, I., Tchkonia, T., Dobson, D. E., Steppan, C. M., Cummins, P., Chan, G., . . .
679 Kirkland, J. L. (2001). Altered expression of C/EBP family members results in
680 decreased adipogenesis with aging. *Am J Physiol Regul Integr Comp Physiol, 280*(6),
681 R1772-1780.
682
683 Komarova, E. A., Antoch, M. P., Novototskaya, L. R., Chernova, O. B., Paszkiewicz, G.,
684 Leontieva, O. V., . . . Gudkov, A. V. (2012). Rapamycin extends lifespan and delays
685 tumorigenesis in heterozygous p53+/- mice. *Aging (Albany NY), 4*(10), 709-714.
686 doi:10.18632/aging.100498
687
688 Lamming, D. W., Ye, L., Katajisto, P., Goncalves, M. D., Saitoh, M., Stevens, D. M., . . . Baur,
689 J. A. (2012). Rapamycin-induced insulin resistance is mediated by mTORC2 loss and
690 uncoupled from longevity. *Science, 335*(6076), 1638-1643.
691 doi:10.1126/science.1215135
692
693 Lee, J. S., Ward, W. O., Ren, H., Vallanat, B., Darlington, G. J., Han, E. S., . . . Corton, J. C.
694 (2012). Meta-analysis of gene expression in the mouse liver reveals biomarkers
695 associated with inflammation increased early during aging. *Mech Ageing Dev, 133*(7),
696 467-478. doi:10.1016/j.mad.2012.05.006
697
698 Liu, J., Ibi, D., Taniguchi, K., Lee, J., Herrema, H., Akosman, B., . . . Ozcan, U. (2016).
699 Inflammation Improves Glucose Homeostasis through IKKbeta-XBP1s Interaction.
700 *Cell, 167*(4), 1052-1066 e1018. doi:10.1016/j.cell.2016.10.015
701

Martin-Montalvo, A., Mercken, E. M., Mitchell, S. J., Palacios, H. H., Mote, P. L., Scheibye-Knudsen, M., . . . de Cabo, R. (2013). Metformin improves healthspan and lifespan in mice. *Nat Commun, 4*, 2192. doi:10.1038/ncomms3192

Mattison, J. A., Roth, G. S., Beasley, T. M., Tilmont, E. M., Handy, A. M., Herbert, R. L., . . . de Cabo, R. (2012). Impact of caloric restriction on health and survival in rhesus monkeys from the NIA study. *Nature, 489*(7415), 318-321. doi:10.1038/nature11432

McCarthy, S. D., Roche, J. F., & Forde, N. (2012). Temporal changes in endometrial gene expression and protein localization of members of the IGF family in cattle: effects of progesterone and pregnancy. *Physiol Genomics, 44*(2), 130-140. doi:10.1152/physiolgenomics.00106.2011

Miller, R. A., Harrison, D. E., Astle, C. M., Baur, J. A., Boyd, A. R., de Cabo, R., . . . Strong, R. (2011). Rapamycin, but not resveratrol or simvastatin, extends life span of genetically heterogeneous mice. *J Gerontol A Biol Sci Med Sci, 66*(2), 191-201. doi:10.1093/gerona/glq178

Mitchell, S. J., Madrigal-Matute, J., Scheibye-Knudsen, M., Fang, E., Aon, M., Gonzalez-Reyes, J. A., . . . de Cabo, R. (2016). Effects of Sex, Strain, and Energy Intake on Hallmarks of Aging in Mice. *Cell Metab, 23*(6), 1093-1112. doi:10.1016/j.cmet.2016.05.027

Müller, C., de Jong, T, Guryev, V, Calkhoven, CF. (2018). *Transcriptome profiling of liver samples of C/EBPβΔuORF mice*. Retrieved from: https://www.ebi.ac.uk/arrayexpress/

Neff, F., Flores-Dominguez, D., Ryan, D. P., Horsch, M., Schroder, S., Adler, T., . . . Ehninger, D. (2013). Rapamycin extends murine lifespan but has limited effects on aging. *J Clin Invest, 123*(8), 3272-3291. doi:10.1172/JCI67674

Park, B. H., Kook, S., Lee, S., Jeong, J. H., Brufsky, A., & Lee, B. C. (2013). An isoform of C/EBPbeta, LIP, regulates expression of the chemokine receptor CXCR4 and modulates breast cancer cell migration. *J Biol Chem, 288*(40), 28656-28667. doi:10.1074/jbc.M113.509505

Raught, B., Gingras, A. C., James, A., Medina, D., Sonenberg, N., & Rosen, J. M. (1996). Expression of a translationally regulated, dominant-negative CCAAT/enhancer-binding protein beta isoform and up-regulation of the eukaryotic translation initiation factor 2alpha are correlated with neoplastic transformation of mammary epithelial cells. *Cancer Res, 56*(19), 4382-4386.

Reimand, J., Arak, T., Adler, P., Kolberg, L., Reisberg, S., Peterson, H., & Vilo, J. (2016). g:Profiler-a web server for functional interpretation of gene lists (2016 update). *Nucleic Acids Res, 44*(W1), W83-89. doi:10.1093/nar/gkw199

Robinson, M. D., McCarthy, D. J., & Smyth, G. K. (2010). edgeR: a Bioconductor package for differential expression analysis of digital gene expression data. *Bioinformatics, 26*(1), 139-140. doi:10.1093/bioinformatics/btp616

Roesler, W. J. (2001). The role of C/EBP in nutrient and hormonal regulation of gene expression. *Annu Rev Nutr, 21*, 141-165. doi:10.1146/annurev.nutr.21.1.141 21/1/141 [pii]

Selman, C., Tullet, J. M., Wieser, D., Irvine, E., Lingard, S. J., Choudhury, A. I., . . . Withers, D. J. (2009). Ribosomal protein S6 kinase 1 signaling regulates mammalian life span. *Science, 326*(5949), 140-144. doi:326/5949/140 [pii] 10.1126/science.1177221

761 Serrano, M. (2016). Unraveling the links between cancer and aging. *Carcinogenesis, 37*(2),
762 107. doi:10.1093/carcin/bgv100
763
764 Singh, P., Coskun, Z. Z., Goode, C., Dean, A., Thompson-Snipes, L., & Darlington, G. (2008).
765 Lymphoid neogenesis and immune infiltration in aged liver. *Hepatology, 47*(5), 1680-
766 1690. doi:10.1002/hep.22224
767
768 Timchenko, L. T., Salisbury, E., Wang, G. L., Nguyen, H., Albrecht, J. H., Hershey, J. W., &
769 Timchenko, N. A. (2006). Age-specific CUGBP1-eIF2 complex increases translation
770 of CCAAT/enhancer-binding protein beta in old liver. *J Biol Chem, 281*(43), 32806-
771 32819. doi:10.1074/jbc.M605701200
772
773 Weindruch, R., & Walford, R. L. (1982). Dietary restriction in mice beginning at 1 year of age:
774 effect on life-span and spontaneous cancer incidence. *Science, 215*(4538), 1415-
775 1418.
776
777 Wethmar, K., Begay, V., Smink, J. J., Zaragoza, K., Wiesenthal, V., Dorken, B., . . . Leutz, A.
778 (2010). C/EBPbetaDeltauORF mice--a genetic model for uORF-mediated
779 translational control in mammals. *Genes Dev, 24*(1), 15-20. doi:24/1/15 [pii]
780 10.1101/gad.557910
781
782 White, R. R., Milholland, B., MacRae, S. L., Lin, M., Zheng, D., & Vijg, J. (2015).
783 Comprehensive transcriptional landscape of aging mouse liver. *BMC Genomics, 16*,
784 899. doi:10.1186/s12864-015-2061-8
785
786 Wilkinson, J. E., Burmeister, L., Brooks, S. V., Chan, C. C., Friedline, S., Harrison, D. E., . . .
787 Miller, R. A. (2012). Rapamycin slows aging in mice. *Aging Cell, 11*(4), 675-682.
788 doi:10.1111/j.1474-9726.2012.00832.x
789
790 Wu, J. J., Liu, J., Chen, E. B., Wang, J. J., Cao, L., Narayan, N., . . . Finkel, T. (2013).
791 Increased Mammalian Lifespan and a Segmental and Tissue-Specific Slowing of
792 Aging after Genetic Reduction of mTOR Expression. *Cell Rep, 4*(5), 913-920.
793 doi:10.1016/j.celrep.2013.07.030
794
795 Zahnow, C. A., Younes, P., Laucirica, R., & Rosen, J. M. (1997). Overexpression of
796 C/EBPbeta-LIP, a naturally occurring, dominant-negative transcription factor, in
797 human breast cancer. *J Natl Cancer Inst, 89*(24), 1887-1891.
798
799 Zaini, M. A., Muller, C., Ackermann, T., Reinshagen, J., Kortman, G., Pless, O., & Calkhoven,
800 C. F. (2017). A screening strategy for the discovery of drugs that reduce C/EBPbeta-
801 LIP translation with potential calorie restriction mimetic properties. *Sci Rep, 7*, 42603.
802 doi:10.1038/srep42603
803
804 Zhang, H. M., Diaz, V., Walsh, M. E., & Zhang, Y. (2017). Moderate lifelong overexpression of
805 tuberous sclerosis complex 1 (TSC1) improves health and survival in mice. *Sci Rep,*
806 *7*(1), 834. doi:10.1038/s41598-017-00970-7
807
808 Zhang, Y., Bokov, A., Gelfond, J., Soto, V., Ikeno, Y., Hubbard, G., . . . Fischer, K. (2014).
809 Rapamycin extends life and health in C57BL/6 mice. *J Gerontol A Biol Sci Med Sci,*
810 *69*(2), 119-130. doi:10.1093/gerona/glt056
811
812 Zidek, L. M., Ackermann, T., Hartleben, G., Eichwald, S., Kortman, G., Kiehntopf, M., . . .
813 Calkhoven, C. F. (2015). Deficiency in mTORC1-controlled C/EBPbeta-mRNA
814 translation improves metabolic health in mice. *EMBO Rep, 16*(8), 1022-1036.
815 doi:10.15252/embr.201439837
816
817

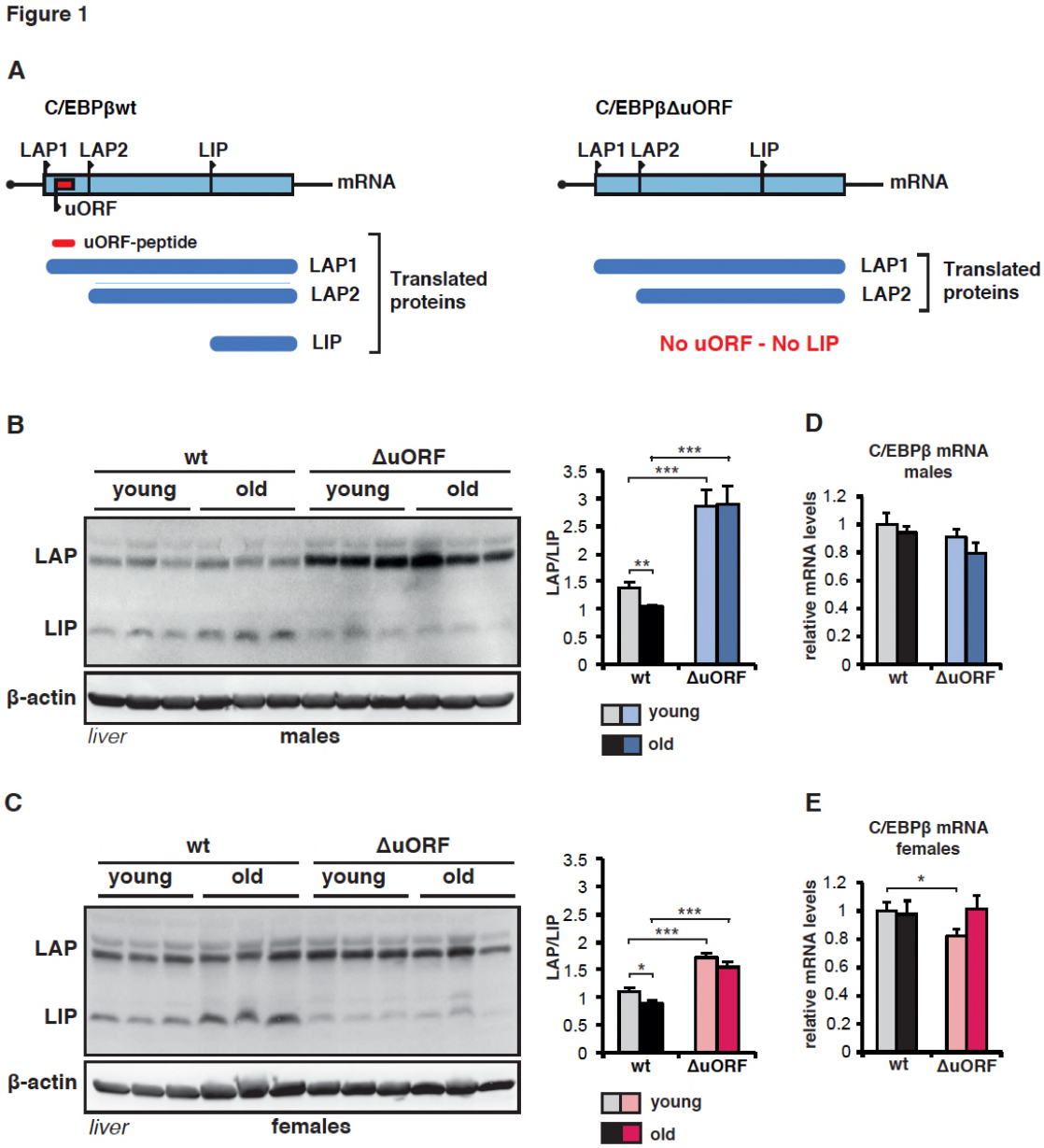

Figure 1. C/EBPβ LAP/LIP isoform ratio increases upon ageing. (A) The graph at the left shows that wt C/EBPβ-mRNA is translated into LAP1 and LAP2 through regular translation initiation, while translation into LIP involves a primary translation of the uORF followed by translation re-initiation at the downstream LIP-AUG by post-uORF-translation ribosomes. The graph at the right shows that genetic ablation of the uORF abolishes translation into LIP, but leaves translation into LAP1 and LAP2 unaffected (for detailed description see(Calkhoven et al., 2000; Zidek et al., 2015). (B and C) Immunoblots of liver samples from young (5 months) and old (female 20 months, male 22 months) wt and C/EBPβ$^{\Delta uORF}$ (B) males and (C) females showing LAP and LIP isoform expression. β-actin expression served as loading control. The LAP/LIP isoform ratio as calculated from quantification by chemiluminescence digital imaging of immunoblots is shown at the right (wt males n=9 young, n=10 old; C/EBPβ$^{\Delta uORF}$ males, n=11 young, n=10 old; wt females, n=9 wt young, n=8 old; C/EBPβ$^{\Delta uORF}$ females, n=10 young, n=10 old). (D) C/EBPβ mRNA levels in males as determined by quantitative real-time PCR (wt, n=11 young, n=11 old; C/EBPβ$^{\Delta uORF}$, n=11 young, n=9 old) and (E) in females (wt, n=9 young, n=11 old; C/EBPβ$^{\Delta uORF}$, n=9 young, n=11 old). P-values were determined by Student's t-test, *p<0.05; **p<0.01; ***p<0.001.

Figure 2

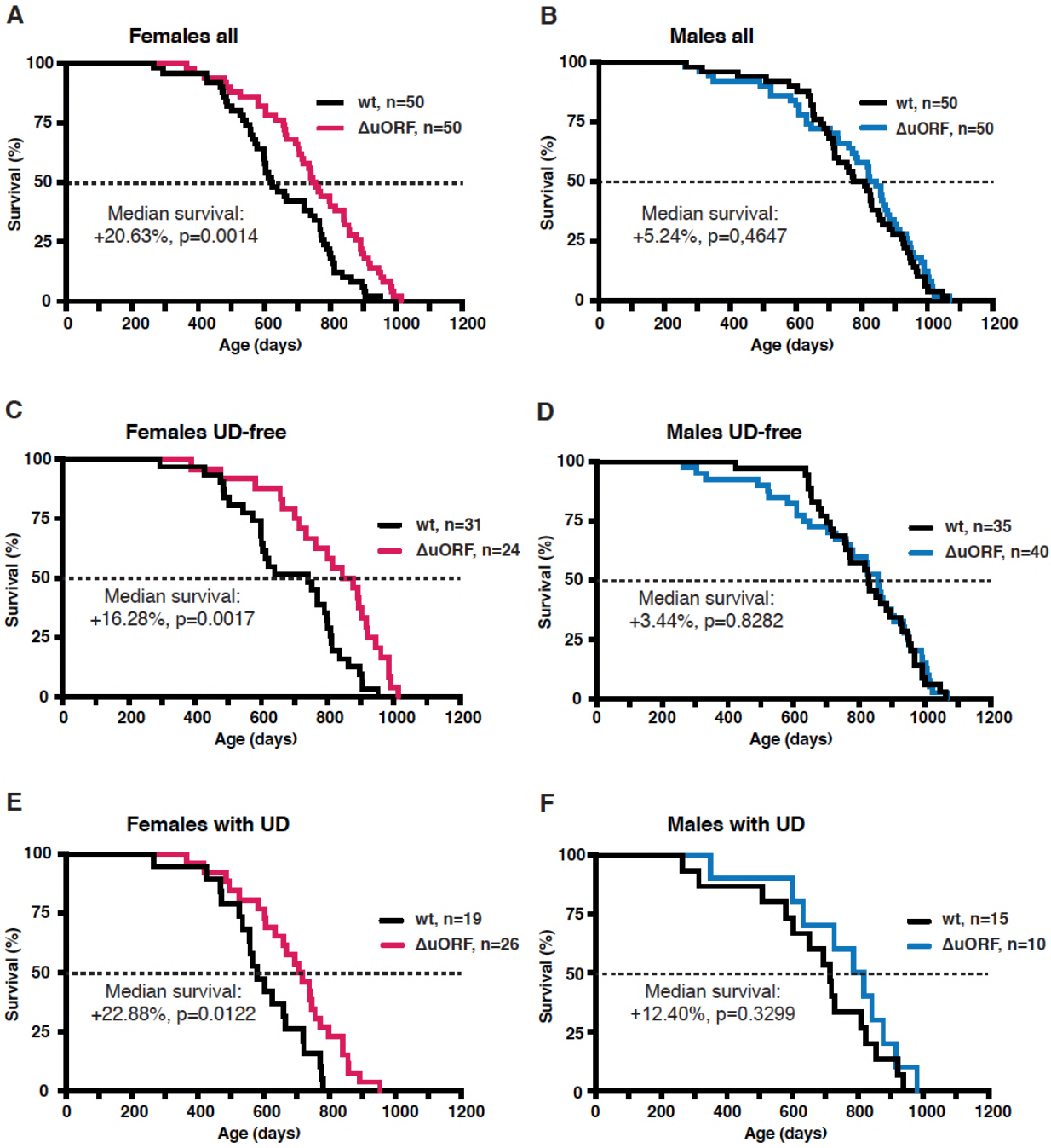

Figure 2. Increased survival of female C/EBPβ$^{\Delta uORF}$ mice. Survival curves of (A) the complete female cohorts, (B) complete male cohorts, (C) the UD-free female cohorts, (D) UD-free male cohorts, (E) female mice with UD and (f) male mice with UD with the survival curves of wt or C/EBPβ$^{\Delta uORF}$ mice indicated. The increase in median survival (%) of C/EBPβ$^{\Delta uORF}$ compared to wt littermates and statistical significance of the increase in the overall survival as determined by the log-rank test is indicated in the figure.

Figure 3

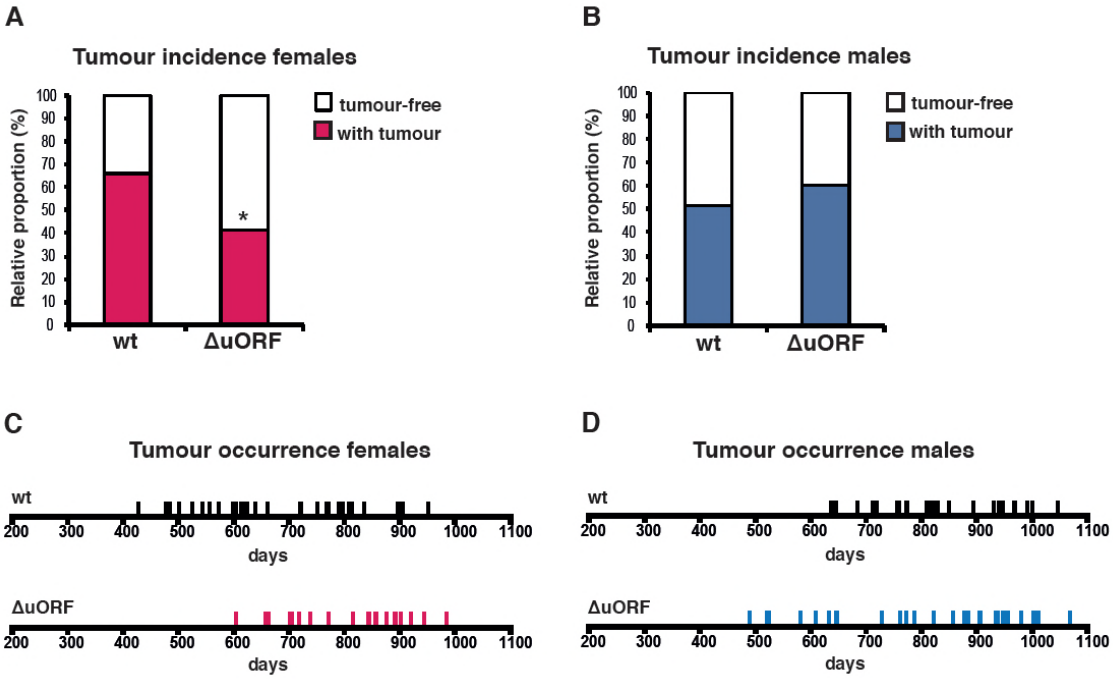

Figure 3. Reduced incidence and delayed occurrence of tumours is female C/EBPβ$^{\Delta uORF}$ mice. (A) Tumour incidence of females as determined by pathological examination of neoplasms found upon necropsy of mice from the lifespan cohorts (wt, n= 50; C/EBPβ$^{\Delta uORF}$, n=48). Statistical significance was calculated using Fisher's exact test with *p<0.05. (B) Tumour incidence of males as determined by pathological examination of neoplasms found upon necropsy (wt, n=47; C/EBPβ$^{\Delta uORF}$, n=45. (C) Tumour occurrence in the female lifespan cohorts upon necropsy is shown for wt (black lines) and C/EBPβ$^{\Delta uORF}$ mice (red lines). (D) Tumour occurrence in the male lifespan cohorts upon necropsy is shown for wt (black lines) and C/EBPβ$^{\Delta uORF}$ mice (blue lines).

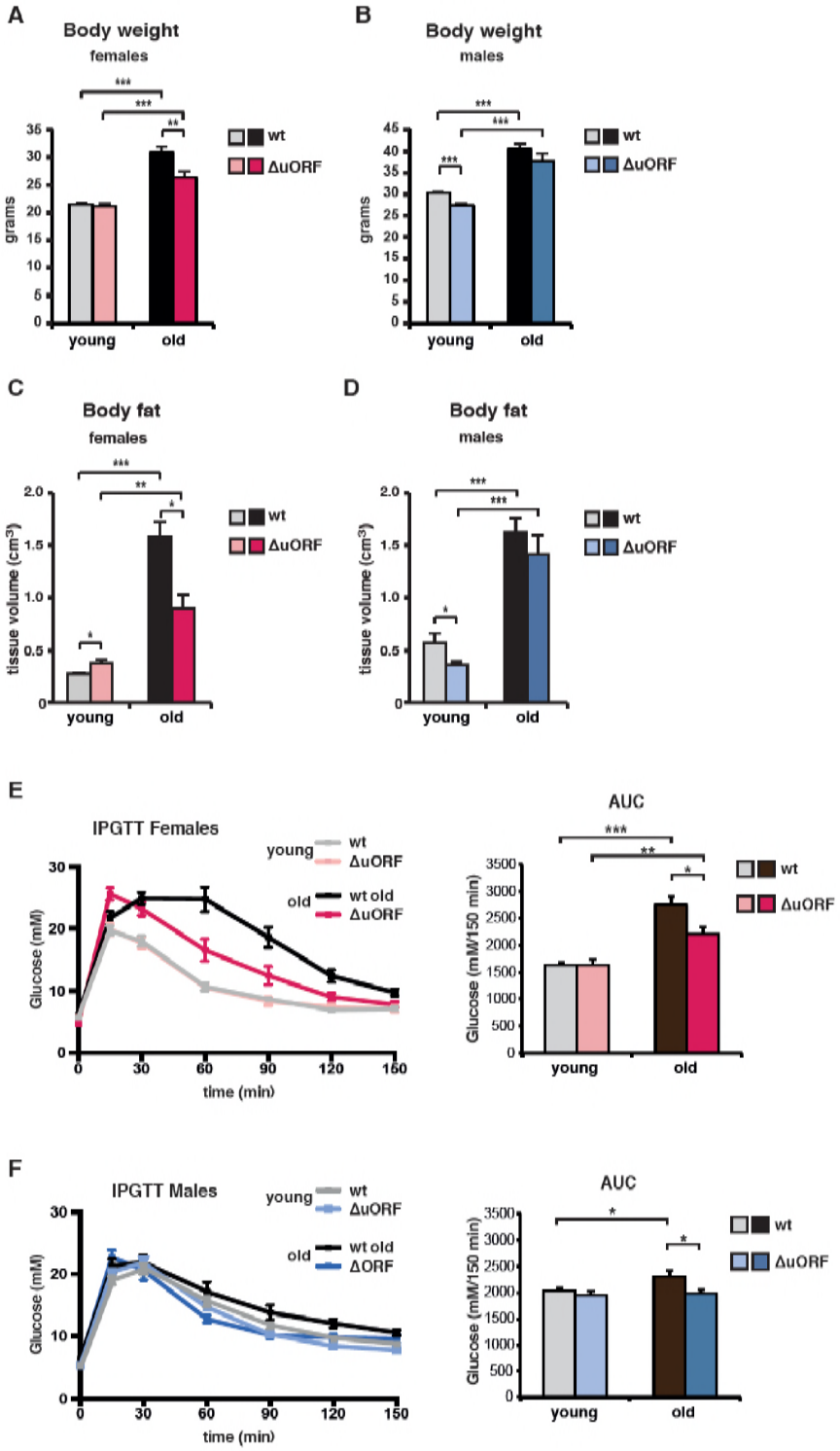

Figure 4. Ageing-associated increase in body weight, fat content and glucose tolerance is attenuated in female C/EBPβ$^{\Delta uORF}$ mice. (A) Body weight (g) of young (4 months) and old (19 months) female mice (wt, n=11 young, n=12 old; C/EBPβ$^{\Delta uORF}$, n=11 young, n=12 old). (B) Body weight of young (4 months) and old (21 months) male mice (wt, n=12 young and old; C/EBPβ$^{\Delta uORF}$, n=12 young, n=11 old). (C) Body fat content (cm^3) as determined by CT analysis of young (4 months) and old (19 months) female mice (wt, n=11 young and old; C/EBPβ$^{\Delta uORF}$, n=9 young, n=11 old). (D) Body fat content of young (4 months) and old (21 months) male mice (wt, n=12 young and old wt; C/EBPβ$^{\Delta uORF}$, n=11 young, n=9 old). (E and F) i.p.-Glucose Tolerance Test (IPGTT) was performed with young (4 months) and old (female 19 months, male 21 months) wt and C/EBPβ$^{\Delta uORF}$ (E) females and (F) males. The area under the curve (AUC) at the right shows the quantification (wt females, n=9 young, n=10 old; C/EBPβ$^{\Delta uORF}$ females, n=10 young, n=11 old; wt males, n=12 young, n=11 old; C/EBPβ$^{\Delta uORF}$ males, n=11 young, n=10 old). P-values were determined by Student's t-test, *p<0.05; **p<0.01; ***p<0.001.

Figure 5

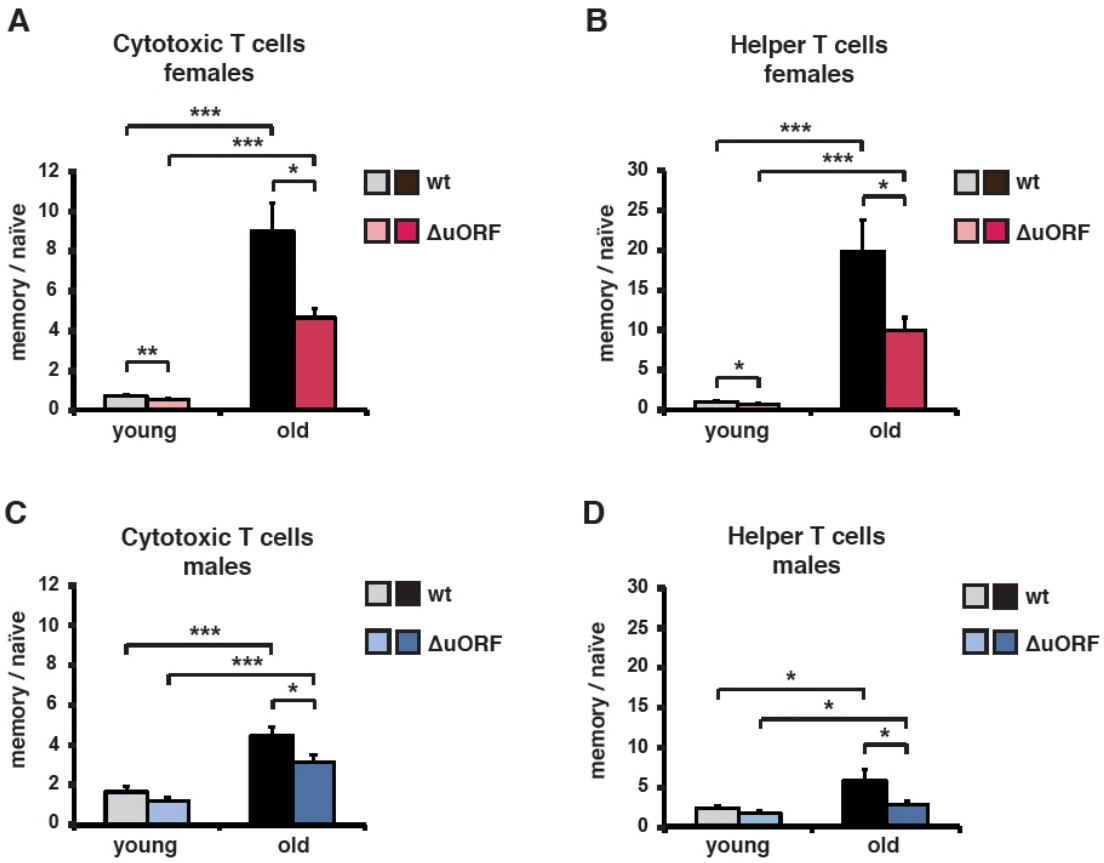

Figure 5. Ageing-associated increase of the memory / naïve T-cell ratio is attenuated in C/EBPβ$^{\Delta uORF}$ mice. The ratio between CD44^{high} memory T cells and CD44^{low}/CD62L^{high} naïve T cells in blood is shown for young (5 months) and old (female 20 months, male 22 months) (A, B) females and (C, D) males for both (a, c) CD8^{+} cytotoxic and (B, D) CD4^{+} helper T cells as was determined by flow cytometry (wt females, n=10 young, n=12 old; wt males n=12 young and old; C/EBPβ$^{\Delta uORF}$ females, n=10 young, n=11 old; C/EBPβ$^{\Delta uORF}$ males, n=12 young and old). P-values were determined by Student's t-test, *p<0.05; ***p<0.001.

Figure 6

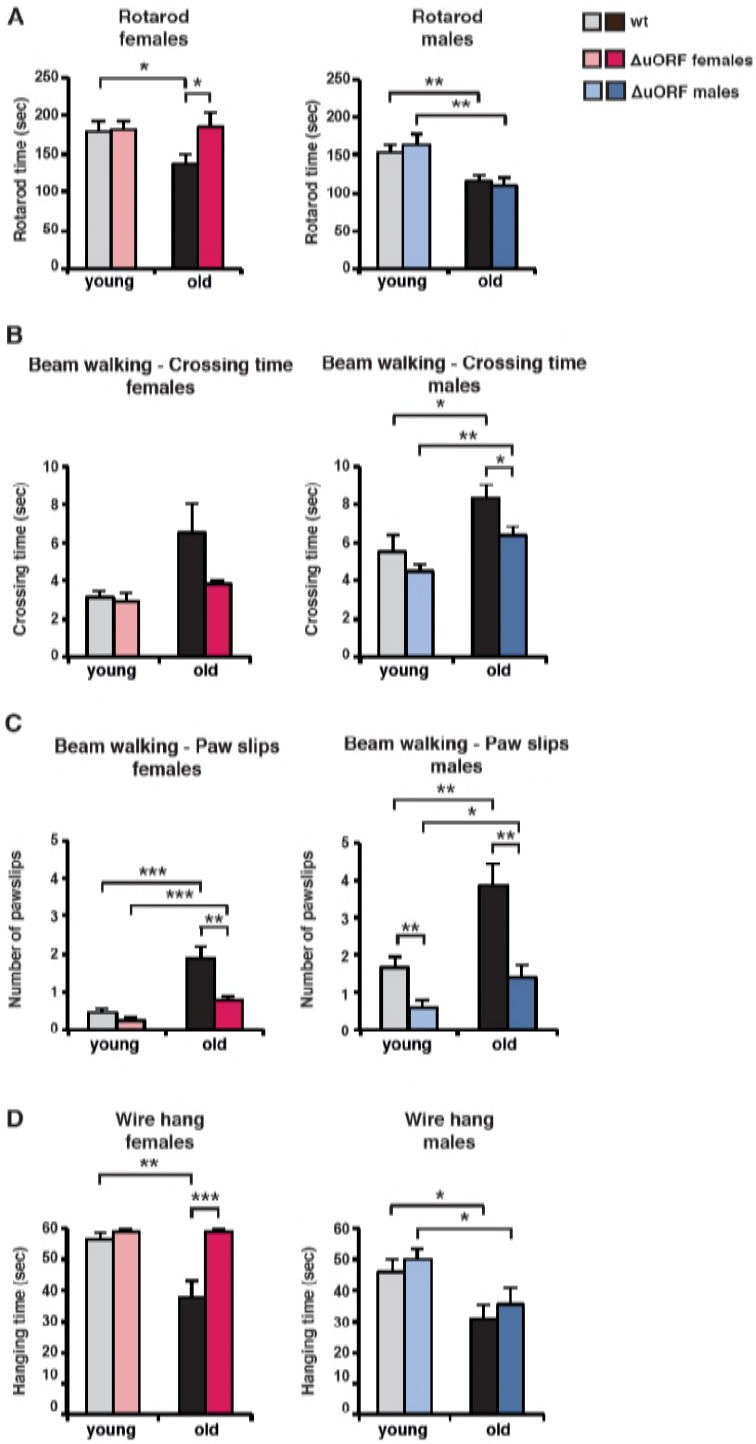

Figure 6. Ageing associated loss of motor coordination and grip strength is attenuated in C/EBPβ$^{\Delta uORF}$ mice. (A) Rotarod performance (time in sec of stay on the rotarod) of young (4 months) and old (female 19 months, male 21 months) wt and C/EBPβ$^{\Delta uORF}$ mice is shown separately for females (left) and males (right) (wt females, n=11 young, n=12 old; wt males, n=12 young and old; C/EBPβ$^{\Delta uORF}$ females, n=11 young, n=12 old; C/EBPβ$^{\Delta uORF}$ males, n=12 young, n=11 old). (B) The crossing time (sec) of the beam walking test of young and old wt and C/EBPβ$^{\Delta uORF}$ mice, and (C) the number of mistakes (paw slips) made while crossing the beam is shown separately for females and males (wt females, n=11 young, n=12 old; wt males, n=12 young and old; C/EBPβ$^{\Delta uORF}$ females, n=11 young, n=12 old; C/EBPβ$^{\Delta uORF}$ males, n=12 young, n=10 old). (D) Grip strength as determined with the wire hang test as hanging time (sec) of young and old wt and C/EBPβ$^{\Delta uORF}$ mice for females and males separately. N=11 for young wt and C/EBPβ$^{\Delta uORF}$ females and for old C/EBPβ$^{\Delta uORF}$ females and n= 12 for old wt females; n=11 for young and old wt males; n=12 for young C/EBPβ$^{\Delta uORF}$ males and n=10 for old C/EBPβ$^{\Delta uORF}$ males. P-values were determined by Student's t-test, *p<0.05; **p<0.01; ***p<0.001.

Figure 7

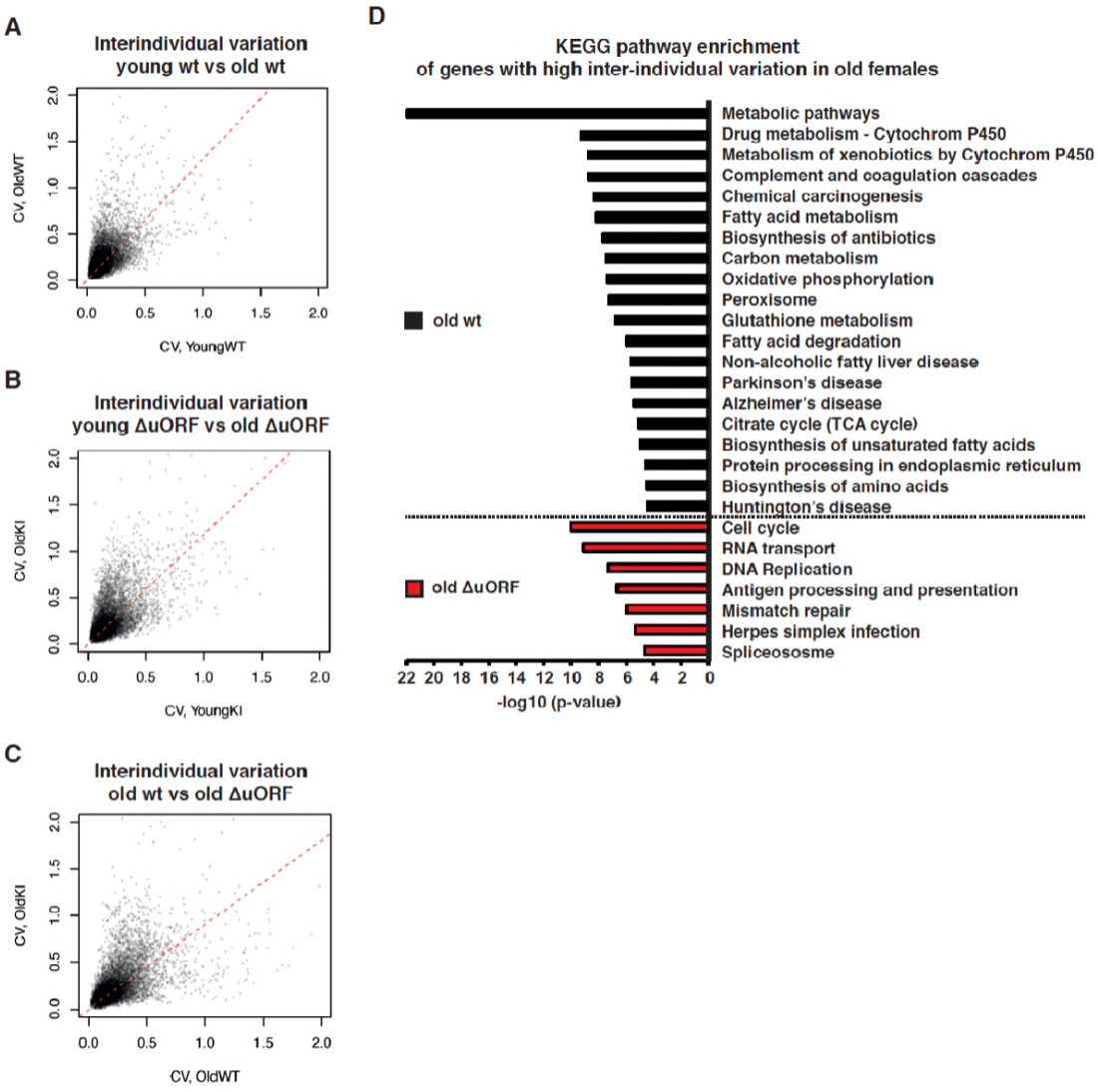

Figure 7. Ageing-associated increase of inter-individual variation of gene expression affects different genes in livers from wt and C/EBPβ$^{\Delta uORF}$ mice. (A-C) Inter-individual variability of liver transcripts compared between (A) young (5 months) versus old (20 months) female wt mice, (B) young (5 months) versus old (20 months) C/EBPβ$^{\Delta uORF}$ female mice and (C) old wt (20 months) versus old C/EBPβ$^{\Delta uORF}$ (20 months) female mice (n=6 for young and old wt and C/EBPβ$^{\Delta uORF}$ for A,B,C). Coefficient of variation of transcripts with mean expression >1 FPM is plotted against the coefficient of variation of the other group as indicated. Dashed red line represents linear regression and is shifted towards the side that shows higher inter-individual variability. (D) KEGG pathway enrichment analysis of genes that show increased inter-individual variability in livers from old wt females compared to old C/EBPβΔuORF females (Coefficient of variation of wt genes is more than twice as the coefficient of variation of the same gene in C/EBPβ$^{\Delta uORF}$ females) as indicated by the black bars or of genes that show increased inter-individual variability in livers from old C/EBPβ$^{\Delta uORF}$ females compared to old wt C/EBPβ$^{\Delta uORF}$ females (Coefficient of variation of C/EBPβ$^{\Delta uORF}$ genes is more than twice as the coefficient of variation of the same gene in wt females) as indicated by the red bars. The x-axis indicates the p-value. Only pathways that show significant enrichment (FDR < 0.05) are shown.

Figure 8

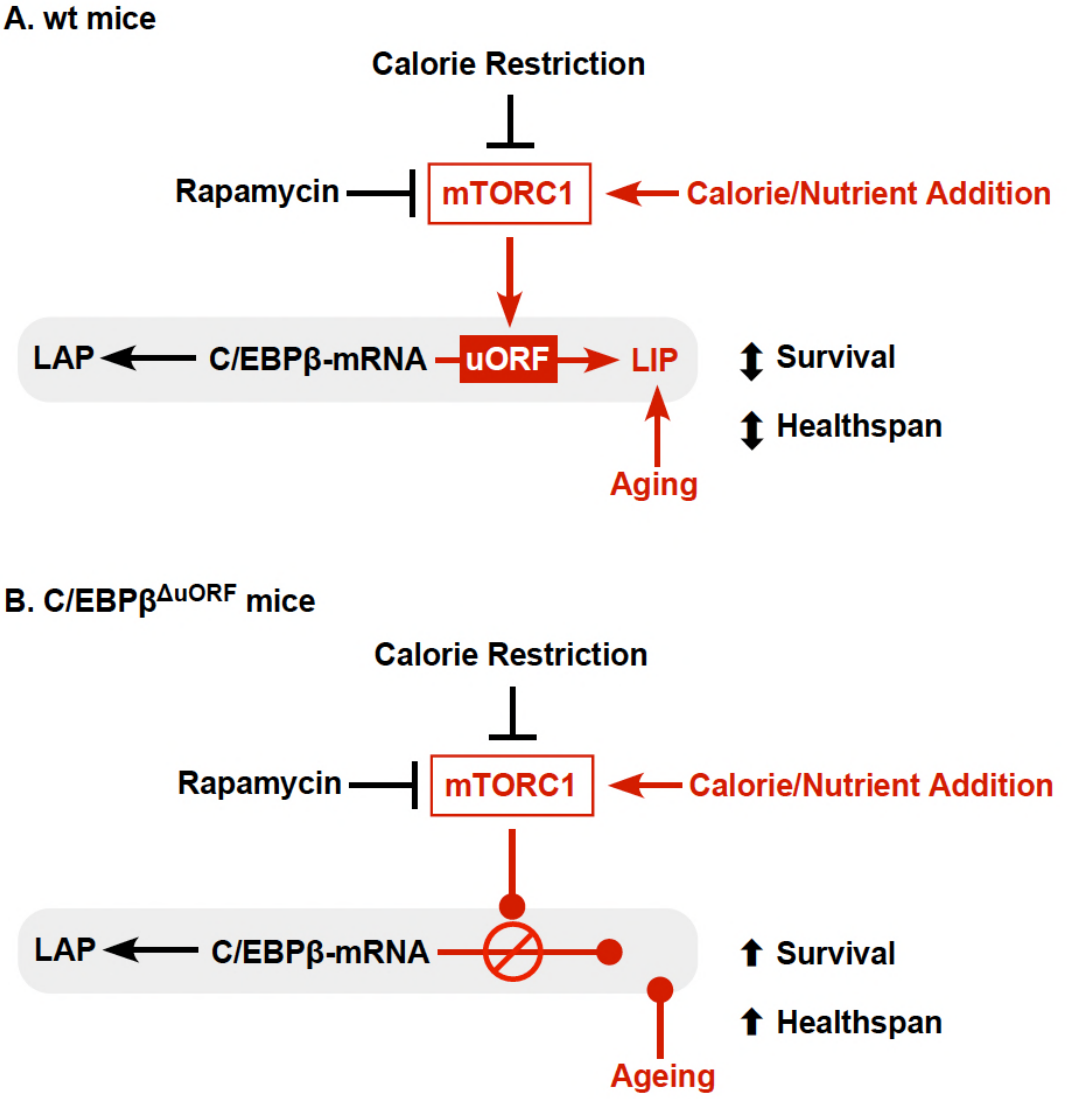

907

908 **Figure 8.** Model explaining regulation of LIP under control of mTORC1. (A) In wt mice
909 C/EBPβ-mRNA translation into LIP is modulated by calorie/nutrient availability through
910 mTORC1 signalling. In addition LIP is upregulated by mechanisms during aging that are not
911 well understood. Expression of LAP is not affected. (B) Deficient expression of LIP in
912 C/EBPβ$^{\Delta uORF}$ mice mimics reduced mTORC1 signalling at the level of C/EBPβ function and
913 prevents the age-associated upregulation of LIP and results in health- and lifespan extension.

Supplement

Figure supplement 1

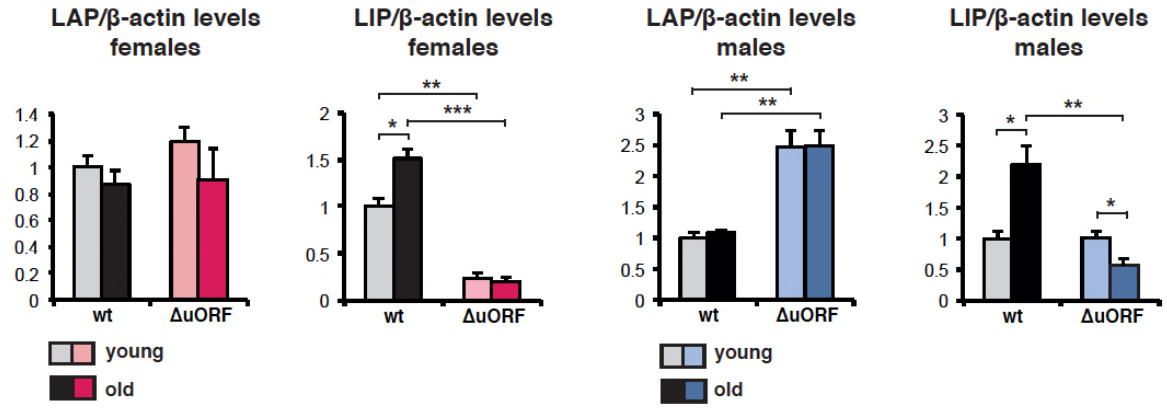

Figure supplement 1. Quantification chemiluminescence digital imaging of LAP or LIP signals in livers in respect to β-actin levels using immunoblots presented in Figure 1A and B and additional immunoblots from young (5 month) and old (female 20 months, male 22 months) mice (wt females, n=9 young and old; wt males, n=10 young, n=11 old; C/EBPβ$^{\Delta uORF}$ females, n=10 young, n=11 old; C/EBPβ$^{\Delta uORF}$ males, n=11 young, n=10 old). P-values were determined by Student's t-test, *p<0.05; **p<0.01; ***p<0.001.

Figure supplement 2

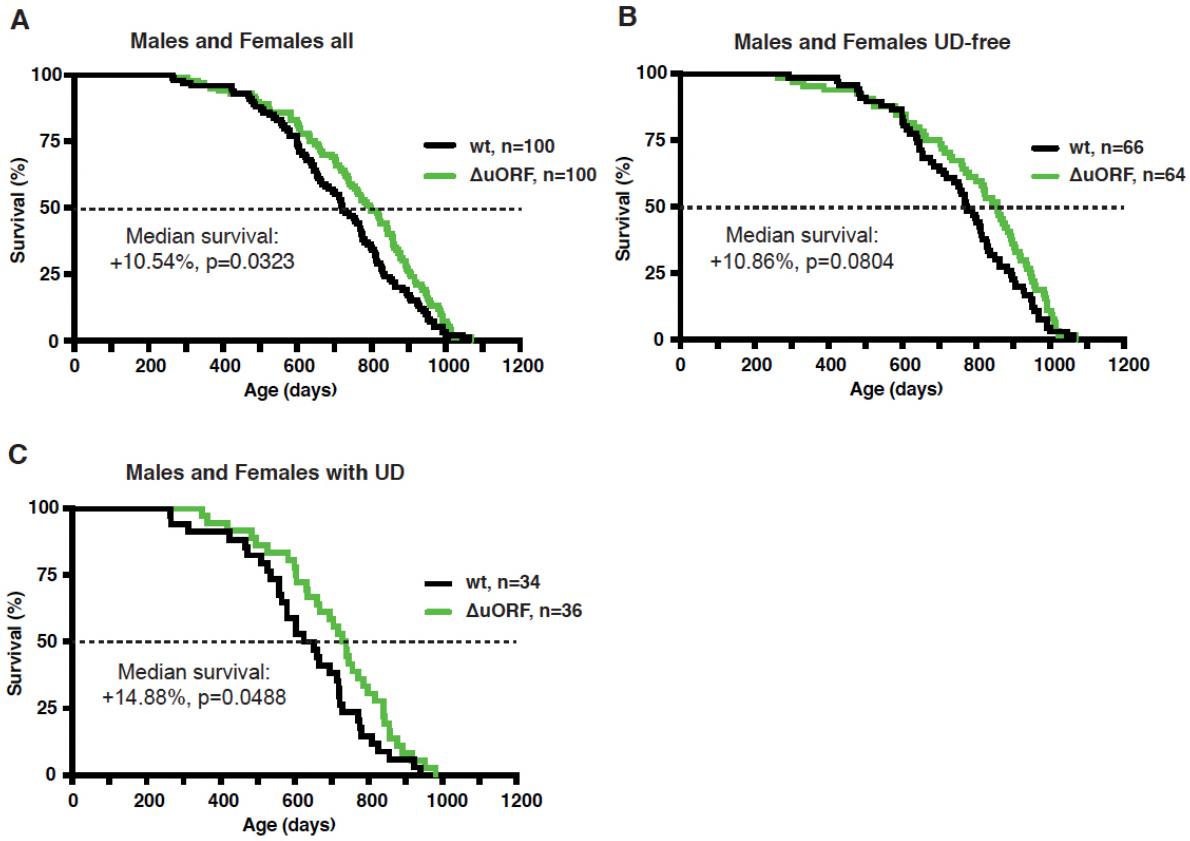

Figure supplement 2. Survival curves of wt and C/EBPβ$^{\Delta uORF}$ mice with females and males combined of (A) the complete cohorts, (B) UD-free mice cohorts and (C) cohorts of mice with UD. For survival curves the increase in median survival (%) of the C/EBPβ$^{\Delta uORF}$ compared to wt mice and statistical significance of the increase in the overall survival as determined by the log-rank test is indicated in the figure.

Figure supplement 3

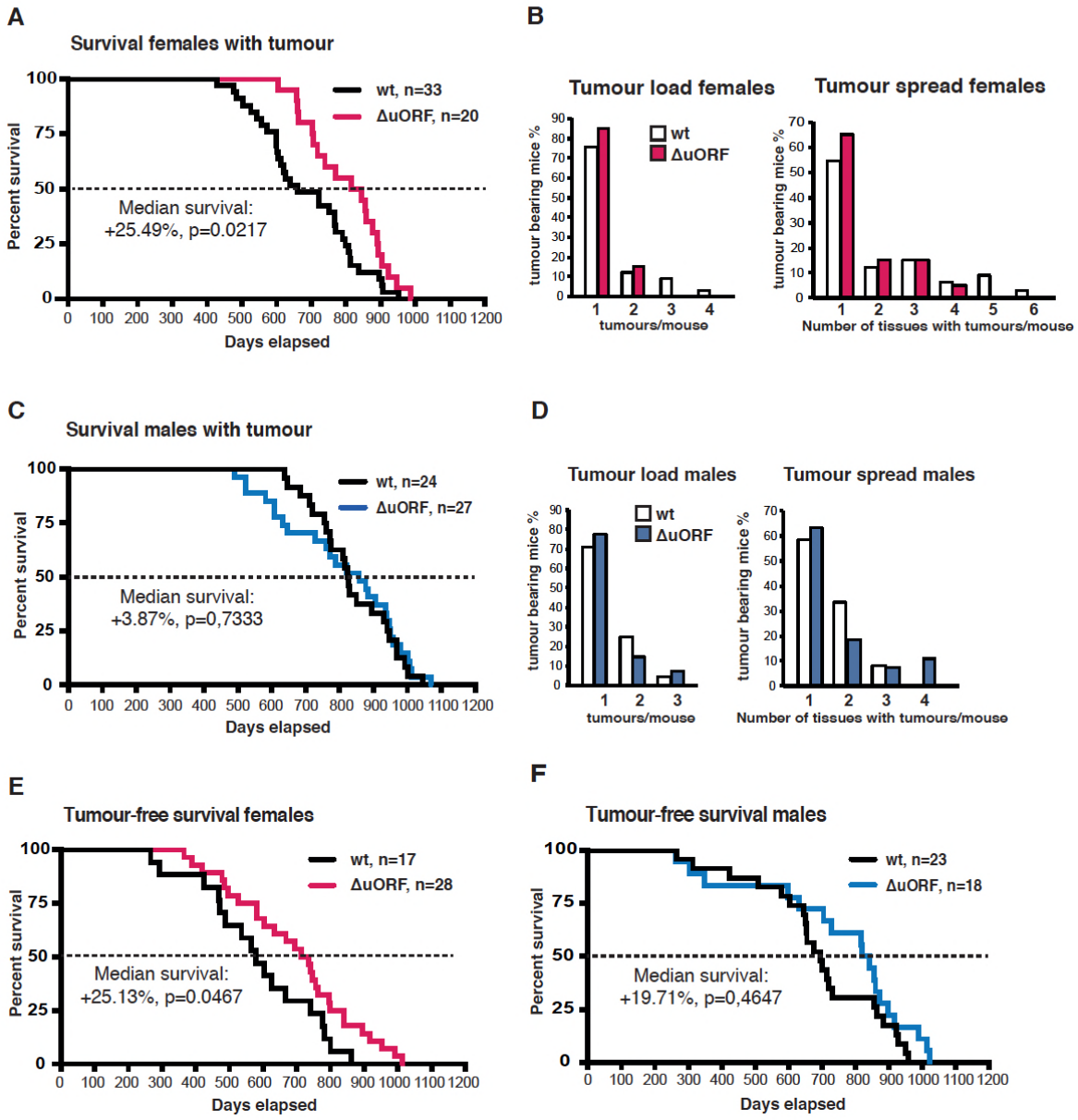

Figure supplement 3.

(A) Survival curves of wt and C/EBPβ$^{\Delta uORF}$ tumour-bearing female mice. (B) At the left, tumour load in wt and C/EBPβ$^{\Delta uORF}$ females as determined by the number of different tumour types found per tumour bearing mouse. At the right, tumour spread in wt and C/EBPβ$^{\Delta uORF}$ females as determined by the number of tissues affected by tumours in tumour bearing mice irrespective of the tumour type (in case different tumour types were found in the same tissue it was counted as >1). (C) Survival curves of wt and C/EBPβ$^{\Delta uORF}$ tumour-bearing male mice. (D) At the left tumour load and at the right tumour spread in wt and C/EBPβ$^{\Delta uORF}$ males as described under (C). (E) Survival curves of wt and C/EBPβ$^{\Delta uORF}$ tumour-free female mice. (F) Survival curves of wt and C/EBPβ$^{\Delta uORF}$ tumour-free male mice. For survival curves the increase in median survival (%) of the C/EBPβ$^{\Delta uORF}$ compared to wt mice and statistical significance of the increase in the overall survival as determined by the log-rank test is indicated in the figure.

Figure supplement 4

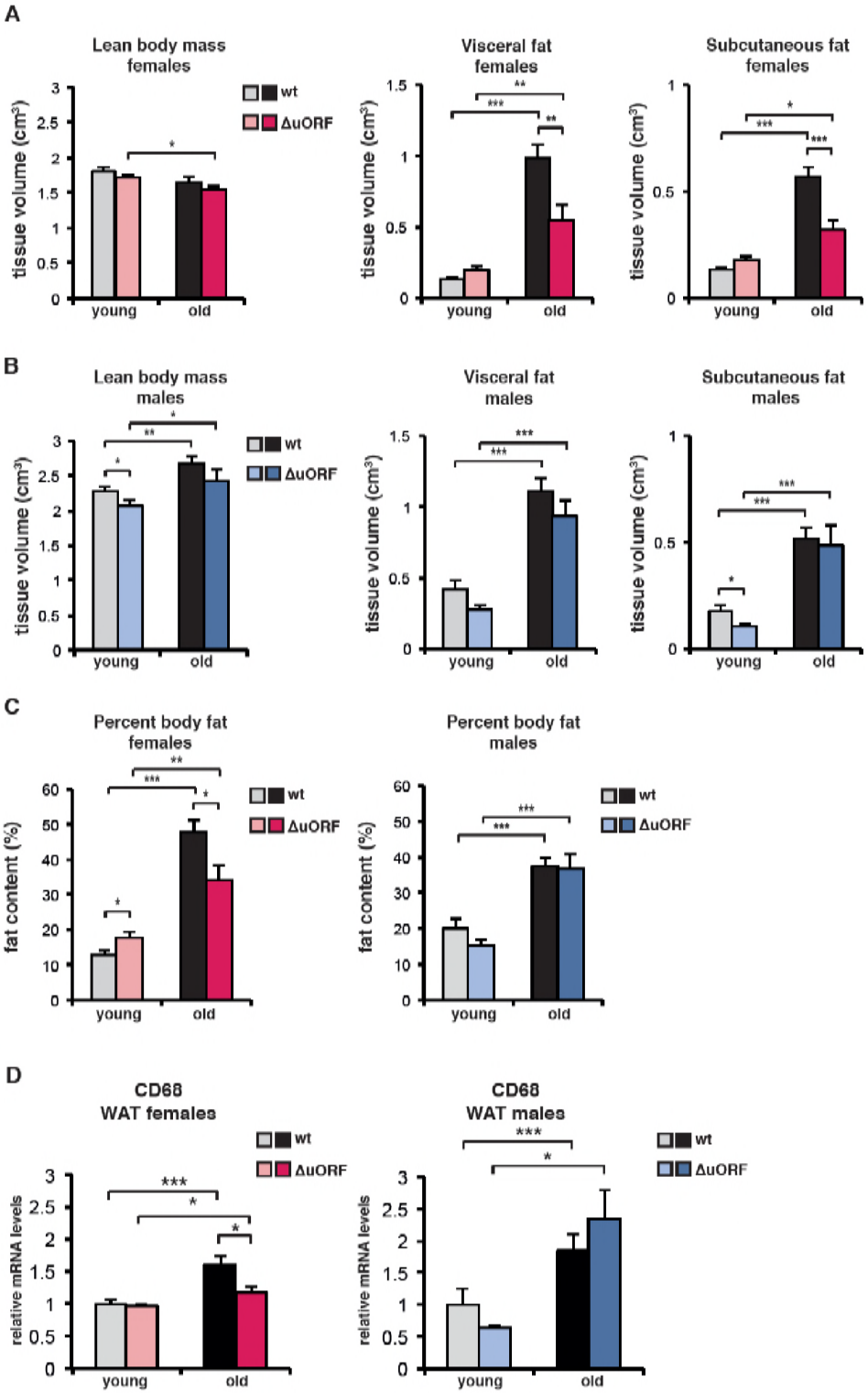

Figure supplement 4. Body composition of young (4 months) and old (females 19 months, males 21 months) wt and C/EBPβ$^{\Delta uORF}$ mice was determined by computer tomography (CT) analysis. (A) The bar graphs show tissue volumes (cm^3) of lean body mass, visceral fat and subcutaneous fat for females, and (B) for males. (C) Percentage of body fat for females (left) or males (right). (wt females, n=11 young and old; wt males, n=12 young and old; C/EBPβ$^{\Delta uORF}$ females, n=9 young, n=11 old; C/EBPβ$^{\Delta uORF}$ males, n=11 young, n=9 old). (d) Relative CD68 mRNA levels as determined by quantitative real-time PCR in visceral fat of young (5 months) and old (females 20 months, males 22 months) wt and C/EBPβ$^{\Delta uORF}$ females (left) and males (right) as a measure for macrophage infiltration (wt females, n=11 young and old; wt males, n=11 young, n=12 old; C/EBPβ$^{\Delta uORF}$ females, n=11 young and old; C/EBPβ$^{\Delta uORF}$ males, n=11 young, n=10 old). P-values were determined by Student's t-test, *p<0.05; **p<0.01; ***p<0.001.

Figure supplement 5

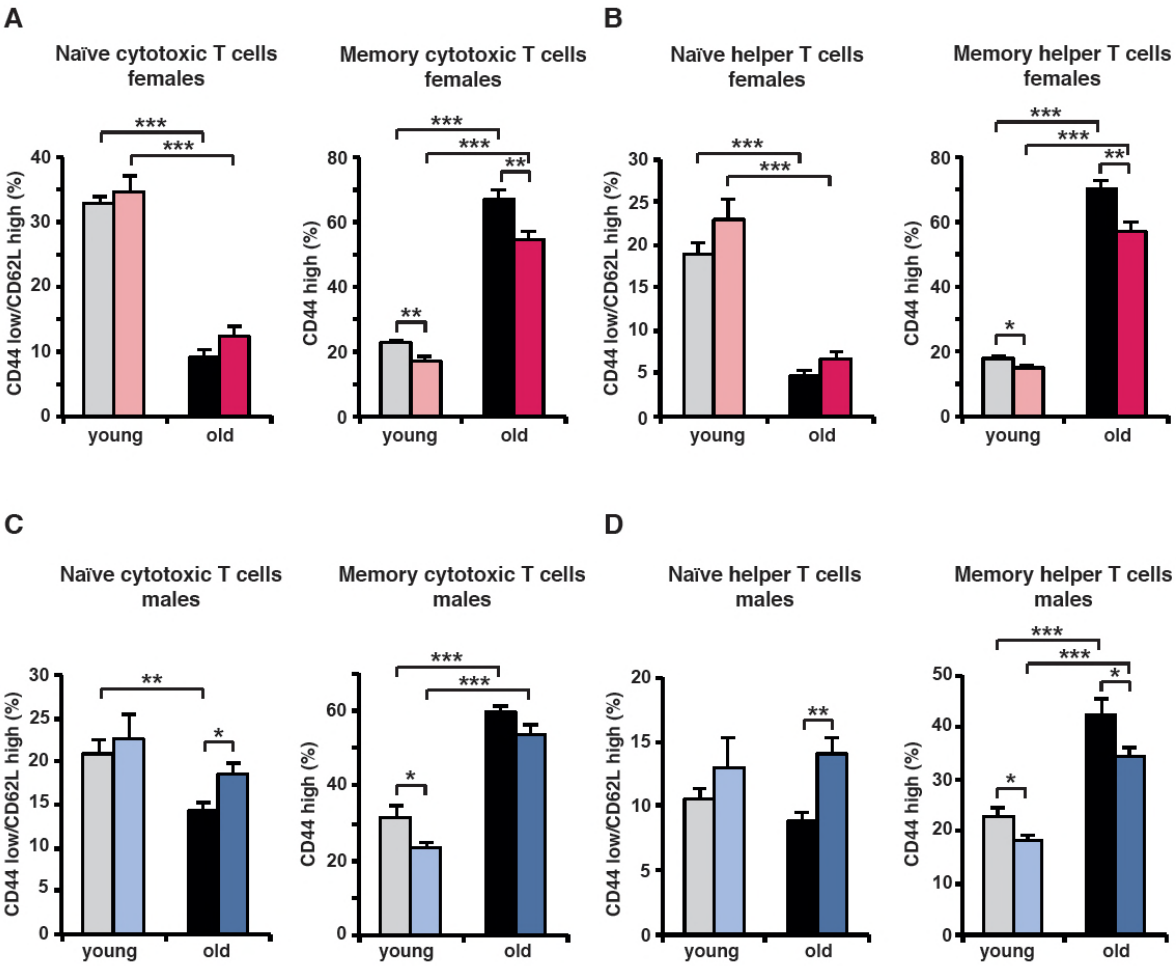

Figure supplement 5. (A) At the left, for females the percentage naïve cytotoxic T cells ($CD44^{low}/CD62L^{high}$) in respect to the total amount of cytotoxic T cells ($CD8^{+}$); at the right, percentage of memory ($CD44^{high}$) cytotoxic T cells in respect to the total amount of cytotoxic ($CD8^{+}$) T cells. (B) At the left, for females the percentage naïve helper T cells ($CD44^{low}/CD62L^{high}$) in respect to the total amount of helper T cells ($CD4^{+}$); at the right percentage memory T cells ($CD44^{high}$) in respect to the total amount of helper T cells ($CD4^{+)}$. (C) The same analysis as in (A) for males. (D) The same analysis as in (B) for males. (wt females, n=10 young, n=12 old; wt males, n=12 young and old; C/EBPβ$^{\Delta uORF}$ females, n=10 young, n=12 old; C/EBPβ$^{\Delta uORF}$ males, n=12 young and old). P-values were determined by Student's t-test, *p<0.05; **p<0.01; ***p<0.001.

Figure supplement 6

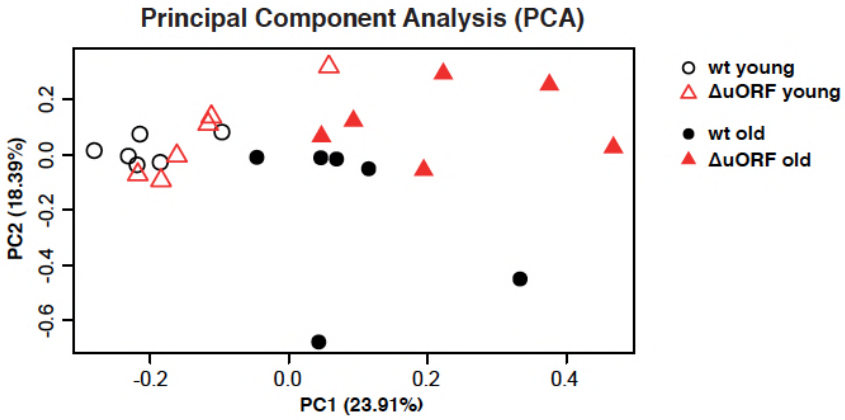

Figure supplement 6. Principal component analysis (PCA) of transcriptome profiles obtained from livers of 5 and 20 months old wt and C/EBPβΔuORF female mice (n=6 for all groups). The main principal component PC1 (x axis, 23,91%) reflects expression changes due to ageing independent of the genotype and the second component PC2 (y axis, 18,39%) reflects expression changes due to the genotype.

Figure supplement 7

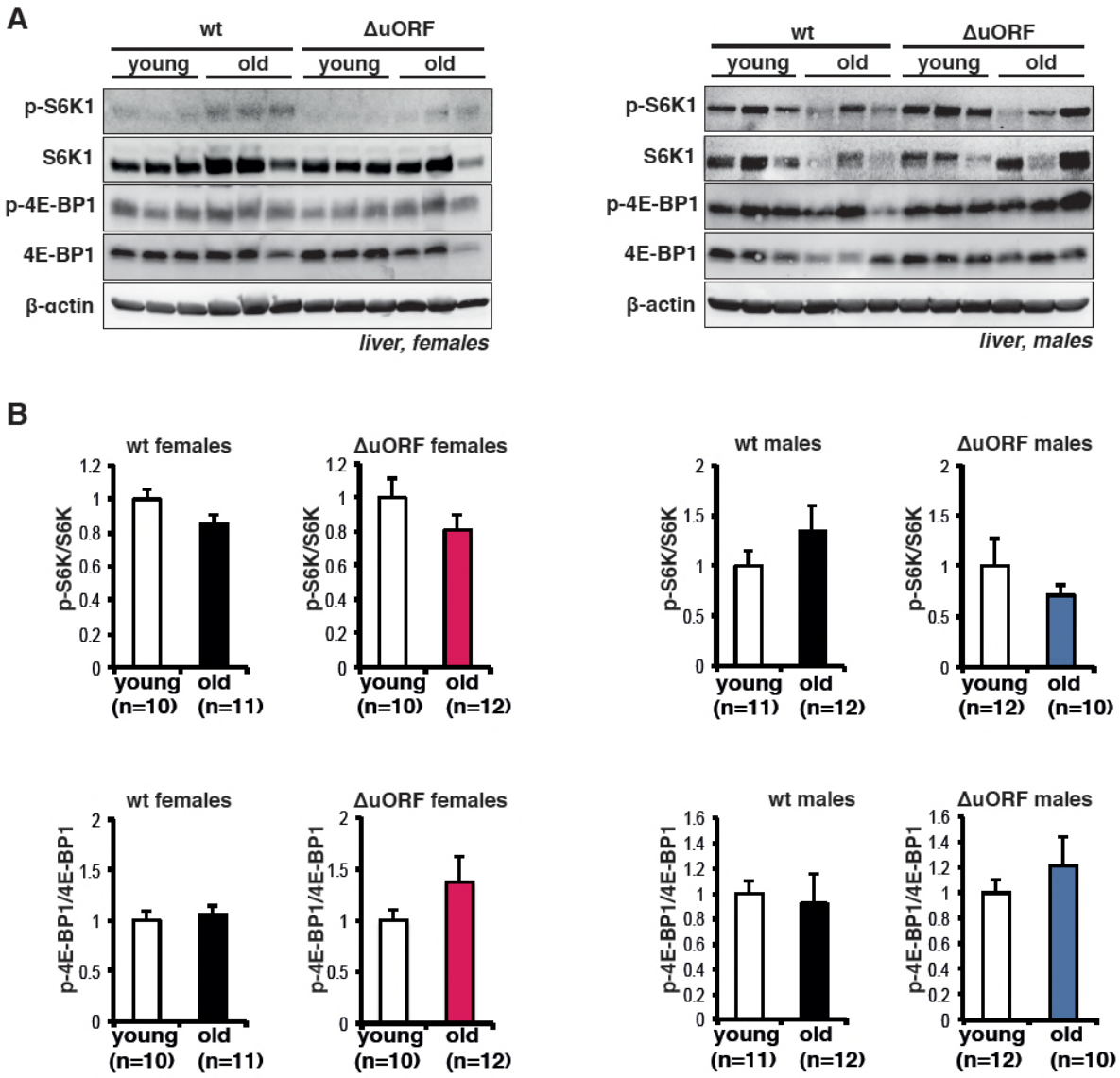

Figure supplement 7. (A) Immunoblots show pan-levels and phosphorylation of the mTORC1 downstream targets S6K1 and 4E-BP1 in liver extracts from young (5 month) and old (females 20 months, males 22 months) of female (left) and male (right) wt and C/EBPβ$^{\Delta uORF}$ mice. β-actin detection served as loading control. (B) Quantification by chemiluminescence digital imaging of phosphorylated proteins in respect to the respective pan levels from the blots presented in (A) and from additional immunoblots (wt females, n=10 young, n=11 old; wt males, n=11 young, n=12 old; C/EBPβ$^{\Delta uORF}$ females, n=10 young, n=12 old; C/EBPβ$^{\Delta uORF}$ males, n=12 young, n=10 old). P-values were determined by Student's t-test, *p<0.05; **p<0.01; ***p<0.001.

Table supplement 1

Lifespan experiment summary of results

Genotype	sex	N[1]	Median[2]	Increase[3]	P_{Surv}[4]	Mean[5]	SEM[6]	N_{max}[7]	P_{max}[8]
All mice									
C/EBPβ$^{\Delta uORF}$	Females	50	751.5	20.63	0.0014	747.42	23.7	9	0.0157
wt	Females	50	623.0			650.96	22.5	1	
C/EBPβ$^{\Delta uORF}$	Males	50	833,5	5.24	0.4647	781.90	28.8	6	0.7407
wt	Males	50	792.0			777.68	24.8	4	
C/EBPβ$^{\Delta uORF}$	Both	100	797.0	10.54	0.0323	764.66	18.6	13	0.2381
wt	Both	100	721.0			714.32	17.8	7	
Mice ulcerative dermatitis (UD)-free									
C/EBPβ$^{\Delta uORF}$	Females	24	860.5	16.28	0.0017	809.29	34.10	5	0.0755
wt	Females	31	740.0			686.07	29.71	1	
C/EBPβ$^{\Delta uORF}$	Males	40	857.5	3.44	0.8282	789.10	33.11	6	0.2710
wt	Males	35	829.0			821.49	24.75	2	
C/EBPβ$^{\Delta uORF}$	Both	64	857.5	10.86	0.0804	796.67	24.19	8	0.3936
wt	Both	66	773.5			757.88	20.78	5	
Mice with UD									
C/EBPβ$^{\Delta uORF}$	Females	26	711.5	22.88	0.0122	690.31	37.37	5	0.0634
wt	Females	19	579.0			593.68	30.65	0	
C/EBPβ$^{\Delta uORF}$	Males	10	802.5	12.40	0.3299	753.1	58.63	1	1.0
wt	Males	15	714.0			675.47	51.28	2	
C/EBPβ$^{\Delta uORF}$	Both	36	733.5	14.88	0.0488	707.75	26.67	5	0.4297
wt	Both	34	638.5			629.77	28.78	2	

[1]Number of animals in the cohort

[2]Median survival of the cohort (days)

[3]Increase of the median survival (percent)

[4]P-value of the increased survival (log-rank test)

[5]Mean lifespan of the cohort (days)

[6]Standard error of the mean

[7]Number of mice in the cohort in the longest-lived decile of the combined cohort (wt and C/EBPβ$^{\Delta uORF}$)

[8]P-value of increased N_{max}[7] (Fisher's exact test)

Table supplement 2

Tumour spectrum in wt and C/EBPβ$^{\Delta uORF}$ mice

Tumour type	Location	wt females	ΔuORF females	wt males	ΔuORF males
Lymphoma *	different	15	6	1	4
Hepatocellular carcinoma	liver	8	4	14	6
Histiocytic sarcoma	liver, colon, intestine, spleen	8	3	14	9
Myeloid neoplasms **	different	4	4	4	6
Adenocarcinoma	pituitary, mammary gland, haderian gland, intestine	2	2	0	3
Bronchio-alveolar carcinoma	lung	0	1	0	3
Mast cell tumour	stomach, liver	1	0	0	1
Anaplastic sarcoma	leg, side	1	1	0	0
Osteosarcoma	leg	1	0	0	0
Undifferentiated sarcoma	pancreas, colon, kidney	0	0	0	1
Squamous cell carcinoma	penis	0	0	1	0
Benign neoplasms	bladder, neck, spleen, liver	3	1	1	0
Unidentified***	liver, kidney, colon, spleen, lung, throat, abdominal cavity, adrenal gland	6	5	3	2

*incl. lymphoid leukaemia
**incl. malignant round cell neoplasms
***tumour type could not be unequivocally determined due to inadequate quality of the fixed tumour tissue

Absolute numbers of mice with the indicated tumour type of tumours found during necropsy for wt and C/EBPβ$^{\Delta uORF}$ males and females are shown. Note that the total number of tumours is higher than the number of tumour-bearing mice due to the eventual occurrence of different tumour types in the same mouse.

Table supplement 3

Occurrence of ageing-associated pathologies in wt and C/EBPβ$^{\Delta uORF}$ mice

Tissue	Pathology/Histology		wt females	ΔuORF females	wt males	ΔuORF males
Liver	Hepatocellular vacuolation	Number[1] Grade[2] ± SEM Significance[3]	9 (9) 1.06 ± 0.19	9 (9) 1.06 ± 0.13	9 (9) 1.5 ± 0.20	9 (9) 0.67 ± 0.12 $p < 0.01$
	Cytoplasmic nuclear inclusions	Number[1] Grade[2] ± SEM Significance[3]	2 (9) 0.06 ± 0.04	2 (9) 0.14 ± 0.11 ns	9 (9) 1.11 ± 0.14	5 (9) 0.33 ± 0.14 $p < 0.01$
	Polyploidy	Number[1] Grade[2] ± SEM Significance[3]	9 (9) 1.39 ± 0.11	9 (9) 1,72 ± 0.17 ns	9 (9) 2.28 ± 0.09	9 (9) 2.06 ± 0.10 ns
	Lymphoplasmatic inflammation	Number[1] Grade[2] ± SEM Significance[3]	4 (9) 0.44 ± 0.19	8 (9) 1.28 ± 0.28 $p < 0.05$	4 (9) 0.39 ± 0.22	7 (9) 0.72 ± 0.21 ns
Pancreas	Islet cell hyperplasia	Number[1] Grade[2] ± SEM Significance[3]	7 (9) 0.72 ± 0.17	4 (9) 0.28 ± 0.12 $p < 0.05$	6 (9) 0.50 ± 0.17	1 (9) 0.06 ± 0.06 $p < 0.05$
	Focal acinar cell atrophy	Number[1] Grade[2] ± SEM Significance[3]	0 (9) 0	2 (9) 0.11 ± 0.07 ns	2 (9) 0.17 ± 0.12	1 (9) 0.06 ± 0.06 ns
	Fatty replacement of acinar cells	Number[1] Grade[2] ± SEM Significance[3]	0 (9) 0	2 (9) 0.17 ± 0.12 ns	2 (9) 0.17 ± 0.12	1 (9) 0.06 ± 0.06 ns
	Inflammation	Number[1] Grade[2] ± SEM Significance[3]	6 (9) 0.39 ± 0.11	7 (9) 0.61 ± 0.16 ns	3 (9) 0.17 ± 0.08	6 (9) 0.33 ± 0.08 ns
Skeletal muscle	Regenerative muscle fibers	Number[1] No.[4] ± SEM Significance[3]	1 (8) 0.13 ± 0.13	3 (9) 0.78 ± 0.55 ns	3 (9) 0.78 ± 0.40	6 (9) 6.33 ± 2.13 $p < 0.05$
	Nuclear condensation	Number[1] Grade[2] ± SEM Significance[3]	3 (9) 0.22 ± 0.12	7 (9) 0.78 ± 0.22 $p < 0.05$	9 (9) 1.22 ± 0.21	7 (9) 1.22 ± 0.28
	Intramuscular adipose tissue	Number[1] Grade[2] ± SEM Significance[3]	6 (9) 2.89 ± 1.11	7 (9) 2.24 ± 1.15 ns	5 (9) 2.82 ± 2.93	6 (9) 8.33 ± 2.92 ns
Spleen	Lymphoid hyperplasia	Number[1] Grade[2] ± SEM Significance[3]	8 (9) 1.83 ± 0.26	9 (9) 1.72 ± 0.12 ns	9 (9) 1.67 ± 0.14	9 (9) 1.72 ± 0.17 ns
	Extramedullary hematopoiesis	Number[1] Grade[2] ± SEM Significance[3]	9 (9) 1.50 ± 0.24	9 (9) 1.06 ± 0.16 ns	9 (9) 1.11 ± 0.14	9 (9) 1.28 ± 0.22 ns
	Dendritic reticular cell hyperplasia	Number[1] Grade[2] ± SEM Significance[3]	4 (9) 0.28 ± 0.12	2 (9) 0.22 ± 0.15 ns	4 (9) 0.22 ± 0.09	4 (9) 0.56 ± 0.28 ns
Skin	Dermal inflammation	Number[1] Grade[2] ± SEM Significance[3]	9 (9) 0.89 ± 0.16	8 (9) 0.44 ± 0.06 $p < 0.05$	9 (9) 0.39 ± 0.04	9 (9) 0.39 ± 0.04
Bone	Bone volume[6]	Bone vol. / tissue vol. (%) ± SEM	0.56 ± 0.11 (n=5)	0.51 ± 0.27 ns (n=5)	3.94 ± 0.42 (n=5)	3.69 ±1.14 ns (n=5)
	Trabecular number[6]	Number (1/μm) ± SEM	$9.00x10^{-5}$ ± $1.48x10^{-5}$ (n=5)	$9,40x10^{-5}$ ± $5.14x10^{-5}$ ns (n=5)	$4.94 x10^{-4}$ ± $5.86x10^{-5}$ (n=5)	$5,66x10^{-4}$ ± $1.75x10^{-4}$ ns (n=5)
	Trabecular thickness[6]	Thickness (μm) ± SEM	62.27 ± 3.97 (n=5)	54,63 ± 10,35 ns (n=5)	80.94 ± 4.58 (n=5)	65.50 ± 1.64 $p < 0.05$ (n=5)
	Trabecular separation[6]	Distance (μm) ± SEM	697,55 ± 48.59 (n=5)	777.81 ± 50.82 ns (n=5)	469.05 ± 36.98 (n=5)	489.07 ± 42.27 ns (n=5)
Blood	IGF-1 levels (plasma)[9]	ng/ml ± SEM Significance[3]	375.4 ± 17.8 (n=11)	321.5 ± 16.4 $p < 0.05$ (n=11)	291.2 ± 21.9 (n=12)	238.6 ± 22.5 ns (n =10)

Mice were part of the ageing cohort and the age at analysis was 20 months for females and 22 months for males.

[1]Number of animals showing the pathology (out of the total number of animals analyzed).

[2]mean grade of the pathology as calculated from the total number of animals analyzed with 0 = absent, 1 = mild, 2 = moderate and 3 = severe.
[3]Statistical significance of difference found between wt and C/EBPβ$^{\Delta uORF}$ mice from the same gender as calculated using the Student's t-test (ns = not significant).
[4]Mean number of regenerating muscle fibers found in five histological tissue slices per mouse. Note that a lower number is an indication for a more progressed ageing phenotype.
[5]mean surface area of intramuscular adipose tissue in percent of the total area of analyzed skeletal muscle tissue as calculated from the total number of animals analyzed.
[6]Trabecular bone parameters (percent bone volume/tissue volume; Trabecular number per mm; trabecular thickness and trabecular separation) measured by micro-CT analysis.

Table supplement 4

GO-term analysis of genes up-regulated in livers of old C/EBPβ$^{\Delta uORF}$ mice

GO term	Description	p-value	FDR	Number of genes	Fold enrich-ment
GO:0009897	External side of plasma membrane	$4.4x10^{-11}$	$5.2x10^{-8}$	16	10.1
GO:0042102	Positive regulation of T cell proliferation	$2.5x10^{-8}$	$3.8x10^{-5}$	8	25.4
GO:0016020	Membrane	$3.9x10^{-8}$	$4.7x10^{-5}$	62	1.8
GO:0031295	T cell costimulation	$1.2x10^{-7}$	$1.8x10^{-4}$	6	48.8
GO:0001772	Immunological synapse	$6.5x10^{-7}$	$7.8x10^{-4}$	6	35.4
GO:0006955	Immune response	$8.1x10^{-7}$	$1.2x10^{-3}$	11	8.2
GO:0042113	B cell activation	$1.1x10^{-5}$	$1.7x10^{-2}$	5	35.0
GO:0046641	Positive regulation of alpha-beta T cell proliferation	$1.8x10^{-5}$	$2.7x10^{-2}$	4	73,9
GO:0045086	Positive regulation of interleukine-2 biosynthetic process	$2.4x10^{-5}$	$3.5x10^{-2}$	4	67.7

Functional annotation of genes upregulated in livers of old C/EBPβ$^{\Delta uORF}$ female mice compared to livers of old wt female mice (FDR < 0.01; 103 from 127 genes; 24 unknown IDs) using the DAVID database (Huang et al., 2009)

Table supplement 5

GO-term analysis of genes down-regulated in livers of old C/EBPβ$^{\Delta uORF}$ mice

GO term	Description	p-value	FDR q-value	Number of genes	Fold enrich-ment
GO:0006953	Acute phase response	$5.3x10^{-6}$	$6.2x10^{-3}$	4	108.8
GO:0005576	Extracellular space	$2.5x10^{-5}$	$2.4x10^{-2}$	9	6.2

Functional annotation of genes downregulated in livers of old C/EBPβ$^{\Delta uORF}$ female mice compared to livers of old wt female mice (FDR < 0.01; 23 from 25 genes, 2 unknown IDs) using the DAVID database (Huang et al., 2009)

Table supplement 6

GO-term analysis of genes showing high inter-individual variation between livers of old wt female mice

GO term	Description	p-value	FDR q-value	Number of genes	Fold enrich-ment
GO:0005739	Mitochondrion	$1.2x10^{-30}$	$1.8x10^{-27}$	236	2.1
GO:0070062	Extracellular exosome	$3.4x10^{-29}$	$5.1x10^{-26}$	315	1.8
GO:0055114	Oxidation-reduction process	$4.4x10^{-26}$	$8.0x10^{-23}$	124	2.8
GO:0005743	Mitochondrial inner membrane	$2.5x10^{-24}$	$3.7x10^{-21}$	86	3.5
GO:0016491	Oxidoreductase activity	$2.6x10^{-24}$	$4.2x10^{-21}$	113	2.8
GO:0005783	Endoplasmic reticulum	$1.8x10^{-17}$	$2.6x10^{-14}$	166	2.0
GO:0008152	Metabolic process	$1.7x10^{-12}$	$3.1x10^{-9}$	74	2.4
GO:0072562	Blood microparticle	$5.0x10^{-11}$	$7.3x10^{-8}$	33	3.9
GO:0006953	Acute phase response	$1.2x10^{-10}$	$2.3x10^{-7}$	17	7.4
GO:0005789	Endoplasmic reticulum membrane	$1.6x10^{-10}$	$2.4x10^{-7}$	92	2.0
GO:0006810	Transport	$2.3x10^{-10}$	$4.2x10^{-7}$	187	1.6
GO:0043231	Intracellular membrane-bounded organelle	$2.9x10^{-10}$	$4.3x10^{-7}$	95	2.0
GO:0007596	Blood coagulation	$2.5x10^{-9}$	$4.5x10^{-6}$	24	4.4

GO:0042730	Fibrinolysis	$3.0x10^{-9}$	$5.6x10^{-6}$	11	11.2
GO:0016020	Membrane	$4.5x10^{-9}$	$6.6x10^{-6}$	546	1.2
GO:0006635	Fatty acid beta-oxidation	$5.9x10^{-8}$	$1.1x10^{-4}$	16	5.6
GO:0006631	Fatty acid metabolic process	$8.0x10^{-8}$	$1.5x10^{-4}$	31	3.0
GO:0031090	Organelle membrane	$8.7x10^{-8}$	$1.3x10^{-4}$	23	3.8
GO:0006629	Lipid metabolic process	$9.2x10^{-8}$	$1.7x10^{-4}$	62	2.1
GO:0007599	Hemostasis	$1.2x10^{-7}$	$2.1x10^{-4}$	16	5.3
GO:0005777	Peroxisome	$2.1x10^{-7}$	$3.1x10^{-4}$	27	3.2
GO:0006749	Glutathione metabolic process	$3.0x10^{-7}$	$5.5x10^{-4}$	16	5.0
GO:0005829	Cytosol	$4.6x10^{-7}$	$6.7x10^{-4}$	167	1.5
GO:0005615	Extracellular space	$9.5x10^{-7}$	$1.4x10^{-3}$	144	1.5
GO:0034364	High-density lipoprotein particle	$2.6x10^{-6}$	$3.8x10^{-3}$	10	7.4
GO:0005793	Endoplasmic reticulum-Golgi intermediate compartment	$4.6x10^{-6}$	$6.7x10^{-3}$	17	3.9
GO:0004364	Glutathione transferase activity	$4.8x10^{-6}$	$7.8x10^{-3}$	12	5.5
GO:0004129	Cytochrome-c oxidase activity	$6.4x10^{-6}$	$1.1x10^{-2}$	11	6.0
GO:0003988	Acetyl-CoA C-acetyltransferase activity	$6.9x10^{-6}$	$1.1x10^{-2}$	6	15.2

GO:0006099	Tricarboxylic acid cycle	$8.7x10^{-6}$	$1.6x10^{-2}$	11	5.8
GO:0020037	Heme binding	$1.1x10^{-5}$	$1.7x10^{-2}$	29	2.5
GO:0043022	Ribosome binding	$1.1x10^{-5}$	$1.8x10^{-2}$	15	4.1
GO:0016829	Lyase activity	$1.2x10^{-5}$	$2.0x10^{-2}$	25	2.7
GO:0005765	Lysosomal membrane	$1.7x10^{-5}$	$2.5x10^{-2}$	34	2.3
GO:0016787	Hydrolase activity	$2.2x10^{-5}$	$3.6x10^{-2}$	142	1.4
GO:0004497	Monooxygenase activity	$2.2x10^{-5}$	$3.6x10^{-2}$	21	3.0

Functional annotation of genes showing a high inter-individual variation between livers from old wt female mice (Coefficient of variation of transcript levels of the corresponding gene in the livers of wt mice is at least twice as big as the coefficient of variation of the transcript levels of the same gene in the livers from C/EBPβ$^{\Delta uORF}$ mice; 1386 from 1414 genes, 28 unknown IDs) using the DAVID database (Huang et al., 2009)

Table supplement 7

GO-term analysis of genes showing high inter-individual variation between livers of old C/EBPβ$^{\Delta uORF}$ female mice

GO term	Description	p-value	FDR q-value	Number of genes	Fold enrich-ment
GO:0005634	Nucleus	$8.9x10^{-45}$	$1.3x10^{-41}$	596	1.6
GO:0005654	Nucleoplasm	$7.1x10^{-35}$	$1.1x10^{-31}$	258	2.2
GO:0007049	Cell cycle	$1.1x10^{-26}$	$2.0x10^{-23}$	116	3.0
GO:0005737	Cytoplasm	$1.4x10^{-25}$	$2.1x10^{-21}$	577	1.4
GO:0003723	Poly(A) RNA binding	$1.8x10^{-20}$	$2.8x10^{-17}$	155	2.2
GO:0005515	Protein binding	$2.4x10^{-16}$	$3.6x10^{-13}$	381	1.4
GO:0006260	DNA replication	$6.1x10^{-17}$	$1.6x10^{-13}$	37	6.1
GO:0000166	Nucleotide binding	$1.2x10^{-14}$	$1.8x10^{-11}$	210	1.7
GO:0051301	Cell division	$2.6x10^{-13}$	$4.8x10^{-10}$	65	2.7
GO:0005524	ATP binding	$2.6x10^{-13}$	$4.2x10^{-10}$	170	1.7
GO:0006351	Transcription, DNA-templated	$1.6x10^{-11}$	$2.9x10^{-8}$	192	1.6
GO:0003677	DNA binding	$3.6x10^{-11}$	$5.8x10^{-8}$	190	1.6
GO:0000278	Mitotic nuclear division	$5.1x10^{-11}$	$9.3x10^{-8}$	50	2.8

GO:0005730	Nucleolus	$6.0x10^{-11}$	$9.1x10^{-8}$	102	2.0
GO:0006974	Cellular response to DNA damage stimulus	$1.4x10^{-10}$	$2.5x10^{-7}$	64	2.4
GO:0003682	Chromatin binding	$1.2x10^{-9}$	$1.9x10^{-6}$	67	2.2
GO:0003723	RNA binding	$5.1x10^{-9}$	$8.1x10^{-6}$	94	1.9
GO:0006281	DNA repair	$6.4x10^{-9}$	$1.2x10^{-5}$	50	2.5
GO:0004386	Helicase activity	$1.0x10^{-8}$	$1.7x10^{-5}$	29	3.5
GO:0006355	Regulation of transcription, DNA templated	$2.7x10^{-8}$	$4.9x10^{-5}$	208	1.4
GO:0002376	Immune system process	$1.6x10^{-7}$	$3.0x10^{-4}$	53	2.2
GO:0005643	Nuclear pore	$2.0x10^{-7}$	$3.0x10^{-4}$	18	4.6
GO:0005694	Chromosome	$2.2x10^{-7}$	$3.3x10^{-4}$	48	2.3
GO:0043234	Protein complex	$2.3x10^{-7}$	$3.4x10^{-4}$	73	1.9
GO:0045893	Positive regulation of transcription, DNA templated	$2.4x10^{-7}$	$4.4x10^{-4}$	70	1.9
GO:0006397	mRNA processing	$4.8x10^{-7}$	$8.9x10^{-4}$	46	2.3
GO:0009615	Response to virus	$9.5x10^{-7}$	$1.7x10^{-3}$	20	3.8
GO:0042393	Histone binding	$1.1x10^{-6}$	$1.7x10^{-3}$	25	3.1
GO:0004402	Histone acetyltransferase activity	$1.4x10^{-6}$	$2.2x10^{-3}$	14	5.2

GO:0008380	RNA splicing	$1.4x10^{-6}$	$2.5x10^{-3}$	37	2.4
GO:0003725	Double-stranded RNA binding	$1.5x10^{-6}$	$2.5x10^{-3}$	18	4.0
GO:0005681	Spliceosomal complex	$2.6x10^{-6}$	$3.9x10^{-3}$	25	3.0
GO:0008283	Cell proliferation	$3.4x10^{-6}$	$6.3x10^{-3}$	34	2.4
GO:0042555	MCM complex	$3.8x10^{-6}$	$5.7x10^{-3}$	7	12.6
GO:0005856	Cytoskeleton	$3.9x10^{-6}$	$5.9x10^{-3}$	107	1.6
GO:0016569	Covalent chromatin modification	$5.5x10^{-6}$	$1.0x10^{-2}$	38	2.3
GO:0030529	Intracellular ribonucleoprotein complex	$6.6x10^{-6}$	$1.0x10^{-2}$	42	2.1
GO:0000122	Negative regulation of transcription from RNA polymerase II promoter	$6.7x10^{-6}$	$1.2x10^{-2}$	78	1.7
GO:0051028	mRNA transport	$8.3x10^{-6}$	$1.5x10^{-2}$	19	3.4
GO:0000281	Mitotic cytokinesis	$9.4x10^{-6}$	$1.7x10^{-2}$	11	5.8
GO:0005813	Centrosome	$1.5x10^{-5}$	$2.2x10^{-2}$	51	1.9
GO:0000775	Chromosome, centromeric region	$1.6x10^{-5}$	$2.4x10^{-2}$	24	2.8
GO:0005829	Cytosol	$1.8x10^{-5}$	$2.7x10^{-2}$	153	1.4
GO:0043967	Histone H4 acetylation	$1.8x10^{-5}$	$3.3x10^{-2}$	11	5.4
GO:0003697	Single-stranded DNA binding	$1.8x10^{-5}$	$2.9x10^{-2}$	18	3.4

GO:0016607	Nuclear speck	$2.3x10^{-5}$	$3.5x10^{-2}$	30	2.4
GO:0005874	Microtubule	$2.5x10^{-5}$	$3.8x10^{-2}$	41	2.0
GO:0000784	Nuclear chromosome, telomeric region	$3.0x10^{-5}$	$4.5x10^{-2}$	22	2.8

Functional annotation of genes showing a high inter-individual variation between livers from old wt female mice (Coefficient of variation of transcript levels of the corresponding gene in the livers of C/EBPβ$^{\Delta uORF}$ mice is at least twice as big as the coefficient of variation of the transcript levels of the same gene in the livers from wt mice; 1354 from 1375 genes, 21 unknown IDs) using the DAVID database (Huang et al., 2009)